Inhomogeneous Hypergraph Clustering with Applications

Pan Li
Department ECE
UIUC
panli2@illinois.edu

Olgica Milenkovic
Department ECE
UIUC
milenkov@illinois.edu

Abstract

Hypergraph partitioning is an important problem in machine learning, computer vision and network analytics. A widely used method for hypergraph partitioning relies on minimizing a normalized sum of the costs of partitioning hyperedges across clusters. Algorithmic solutions based on this approach assume that different partitions of a hyperedge incur the same cost. However, this assumption fails to leverage the fact that different subsets of vertices within the same hyperedge may have different structural importance. We hence propose a new hypergraph clustering technique, termed inhomogeneous hypergraph partitioning, which assigns different costs to different hyperedge cuts. We prove that inhomogeneous partitioning produces a quadratic approximation to the optimal solution if the inhomogeneous costs satisfy submodularity constraints. Moreover, we demonstrate that inhomogenous partitioning offers significant performance improvements in applications such as structure learning of rankings, subspace segmentation and motif clustering.

1 Introduction

Graph partitioning or clustering is a ubiquitous learning task that has found many applications in statistics, data mining, social science and signal processing [1, 2]. In most settings, clustering is formally cast as an optimization problem that involves entities with different pairwise similarities and aims to maximize the total "similarity" of elements within clusters [3, 4, 5], or simultaneously maximize the total similarity within cluster and dissimilarity between clusters [6, 7, 8]. Graph partitioning may be performed in an agnostic setting, where part of the optimization problem is to automatically learn the number of clusters [6, 7].

Although similarity among entities in a class may be captured via pairwise relations, in many real-world problems it is necessary to capture joint, higher-order relations between subsets of objects. From a graph-theoretic point of view, these higher-order relations may be described via hypergraphs, where objects correspond to vertices and higher-order relations among objects correspond to hyperedges. The vertex clustering problem aims to minimize the similarity across clusters and is referred to as hypergraph partitioning. Hypergraph partitioning has found a wide range of applications in network motif clustering, subspace clustering and image segmentation. [8, 9, 10, 11, 12].

Classical hypergraph partitioning approaches share the same setup: A nonnegative weight is assigned to every hyperedge and if the vertices in the hyperedge are placed across clusters, a cost proportional to the weight is charged to the objective function [13]. We refer to this clustering procedure as *homogenous hyperedge clustering* and refer to the corresponding partition as a *homogeneous partition (H-partition)*. Clearly, this type of approach prohibits the use of information regarding how different vertices or subsets of vertices belonging to a hyperedge contribute to the higher-order relation. A more appropriate formulation entails charging different costs to different cuts of the hyperedges, thereby endowing hyperedges with vector weights capturing these costs. To illustrate the point,
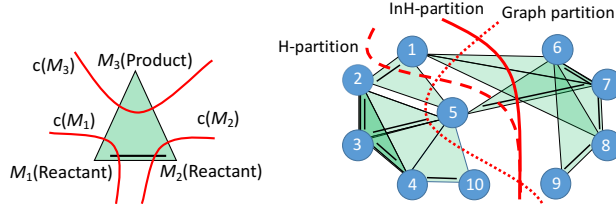
Figure 1: Clusters obtained using homogenous and inhomogeneous hypergraph partitioning and graph partitioning (based on pairwise relations). Left: Each reaction is represented by a hyperedge. Three different cuts of a hyperedge are denoted by $c(M_3), c(M_1)$, and $c(M_2)$, based on which vertex is "isolated" by the cut. The graph partition only takes into account pairwise relations between reactants, corresponding to $w(c(M_3)) = 0$. The homogenous partition enforces the three cuts to have the same weight, $w(c(M_3)) = w(c(M_1)) = w(c(M_2))$, while an inhomogenous partition is not required to satisfy this constraint. Right: Three different clustering results based on optimally normalized cuts for a graph partition, a homogenous partition (H-partition) and an inhomogenous partition (InH-partition) with $0.01w(c(M_1)) \leq w(c(M_3)) \leq 0.44w(c(M_1))$.

consider the example of metabolic networks [14]. In these networks, vertices describe metabolites while edges describe transformative, catalytic or binding relations. Metabolic reactions are usually described via equations that involve more than two metabolites, such as $M_1 + M_2 \rightarrow M_3$. Here, both metabolites M_1 and M_2 need to be present in order to complete the reaction that leads to the creation of the product M_3. The three metabolites play different roles: M_1, M_2 are reactants, while M_3 is the product metabolite. A synthetic metabolic network involving reactions with three reagents as described above is depicted in Figure 1, along with three different partitions induced by a homogeneous, inhomogeneous and classical graph cut. As may be seen, the hypergraph cuts differ in terms of how they split or group pairs of reagents. The inhomogeneous clustering preserves all but on pairing, while the homogenous clustering splits two pairings. The graph partition captures only pairwise relations between reactants and hence, the optimal normalized cut over the graph splits six reaction triples. The differences between inhomogenous, homogenous, and pairwise-relation based cuts are even more evident for large graphs and they may lead to significantly different partitioning performance in a number of important partitioning applications.

The problem of inhomogeneous hypergraph clustering has not been previously studied in the literature. The main results of the paper are efficient algorithms for inhomogeneous hypergraph partitioning with theoretical performance guarantees and extensive testing of inhomogeneous partitioning in applications such as hierarchical biological network studies, structure learning of rankings and subspace clustering (All proofs and discussions of some applications are relegated to the Supplementary Material). The algorithmic methods are based on transforming hypergraphs into graphs and subsequently performing spectral clustering based on the normalized Laplacian of the derived graph. A similar approach for homogenous clustering has been used under the name of Clique Expansion [11]. However, the projection procedure, which is the key step of Clique Expansion, differs significantly from the projection procedure used in our work, as the inhomogenous clustering algorithm allows non-uniform expansion of one hyperedge while Clique Expansion only allows for uniform expansions. A straightforward analysis reveals that the normalized hypergraph cut problem [13] and the normalized Laplacian homogeneous hypergraph clustering algorithms [10, 13] are special cases of our proposed algorithm, where the costs assigned to the hyperedges take a very special form. Furthermore, we show that when the costs of the proposed inhomogeneous hyperedge clustering are *submodular*, the projection procedure is guaranteed to find a constant-approximation solutions for several graph-cut related entities. Hence, the inhomogeneous clustering procedure has the same quadratic approximation properties as spectral graph clustering [15].

2 Preliminaries and Problem Formulation

A hypergraph $\mathcal{H} = (V, E)$ is described in terms of a vertex set $V = \{v_1, v_2, ..., v_n\}$ and a set of hyperedges E. A hyperedge $e \in E$ is a subset of vertices in V. For an arbitrary set S, we let $|S|$ stand for the cardinality of the set, and use $\delta(e) = |e|$ to denote the size of a hyperedge. If for all $e \in E$, $\delta(e)$ equals a constant Δ, the hypergraph is called a Δ-uniform hypergraph.

Let 2^e denote the power set of e. An inhomogeneous hyperedge (InH-hyperedge) is a hyperedge with an associated weight function $w_e : 2^e \rightarrow \mathbb{R}_{\geq 0}$. The weight $w_e(S)$ indicates the cost of cutting/partitioning the hyperedge e into two subsets, $\bar{S}$ and e/S. A consistent weight $w_e(S)$ satisfies

the following properties: $w_e(\emptyset) = 0$ and $w_e(S) = w_e(e/S)$. The definition also allows $w_e(\cdot)$ to be enforced only for a subset of 2^e. However, for singleton sets $S = \{v\} \in e$, $w_e(\{v\})$ has to be specified. The degree of a vertex v is defined as $d_v = \sum_{e: v \in e} w_e(\{v\})$, while the volume of a subset of vertices $S \subseteq V$ is defined as

$$\text{vol}_{\mathcal{H}}(S) = \sum_{v \in S} d_v. \tag{1}$$

Let $(S, \bar{S})$ be a partition of the vertices V. Define the hyperedge boundary of S as $\partial S = \{e \in E | e \cap S \neq \emptyset, e \cap \bar{S} \neq \emptyset\}$ and the corresponding set volume as

$$\text{vol}_{\mathcal{H}}(\partial S) = \sum_{e \in \partial S} w_e(e \cap S) = \sum_{e \in E} w_e(e \cap S), \tag{2}$$

where the second equality holds since $w_e(\emptyset) = w_e(e) = 0$. The task of interest is to minimize the *normalized cut* NCut of the hypergraph with InH-hyperedges, i.e., to solve the following optimization problem

$$\arg\min_S \text{NCut}_{\mathcal{H}}(S) = \arg\min_S \text{vol}_{\mathcal{H}}(\partial S) \left(\frac{1}{\text{vol}_{\mathcal{H}}(S)} + \frac{1}{\text{vol}_{\mathcal{H}}(\bar{S})} \right). \tag{3}$$

One may also extend the notion of InH hypergraph partitioning to k-way InH-partition. For this purpose, we let $(S_1, S_2, ..., S_k)$ be a k-way partition of the vertices V, and define the k-way normalized cut for inH-partition according to

$$\text{NCut}_{\mathcal{H}}(S_1, S_2, ..., S_k) = \sum_{i=1}^{k} \frac{\text{vol}_{\mathcal{H}}(\partial S_i)}{\text{vol}_{\mathcal{H}}(S_i)}. \tag{4}$$

Similarly, the goal of a k-way inH-partition is to minimize $\text{NCut}_{\mathcal{H}}(S_1, S_2, ..., S_k)$. Note that if $\delta(e) = 2$ for all $e \in E$, the above definitions are consistent with those used for graphs [16].

3 Inhomogeneous Hypergraph Clustering Algorithms

Motivated by the homogeneous clustering approach of [11], we propose an inhomogeneous clustering algorithm that uses three steps: 1) Projecting each InH-hyperedge onto a subgraph; 2) Merging the subgraphs into a graph; 3) Performing classical spectral clustering based on the normalized Laplacian (described in the Supplementary Material, along with the complexity of all algorithmic steps). The novelty of our approach is in introducing the inhomogenous clustering constraints via the projection step, and stating an optimization problem that provides the provably best weight splitting for projections. All our theoretical results are stated for the NCut problem, but the proposed methods may be used as heuristics for k-way NCuts.

Suppose that we are given a hypergraph with inhomogeneous hyperedge weights, $\mathcal{H} = (V, E, \mathbf{w})$. For each InH-hyperedge (e, w_e), we aim to find a complete subgraph $G_e = (V^{(e)}, E^{(e)}, w^{(e)})$ that "best" represents this InH-hyperedge; here, $V^{(e)} = e$, $E^{(e)} = \{\{v, \tilde{v}\} | v, \tilde{v} \in e, v \neq \tilde{v}\}$, and $w^{(e)} : E^{(e)} \to R$ denotes the hyperedge weight vector. The goal is to find the graph edge weights that provide the best approximation to the split hyperedge weight according to:

$$\min_{w^{(e)}} \beta^{(e)} \text{ s.t. } w_e(S) \leq \sum_{v \in S, \tilde{v} \in e/S} w_{v\tilde{v}}^{(e)} \leq \beta^{(e)} w_e(S), \text{ for all } S \in 2^e \text{ s.t. } w_e(S) \text{ is defined.} \tag{5}$$

Upon solving for the weights $w^{(e)}$, we construct a graph $\mathcal{G} = (V, E_o, w)$, where V are the vertices of the hypergraph, E_o is the complete set of edges, and where the weights $w_{v\tilde{v}}$, are computed via

$$w_{v\tilde{v}} \triangleq \sum_{e \in E} w_{v\tilde{v}}^{(e)}, \quad \forall \{v, \tilde{v}\} \in E_o. \tag{6}$$

This step represents the projection weight merging procedure, which simply reduces to the sum of weights of all hyperedge projections on a pair of vertices. Due to the linearity of the volumes (1) and boundaries (2) of sets S of vertices, for any $S \subset V$, we have

$$\text{Vol}_{\mathcal{H}}(\partial S) \leq \text{Vol}_{\mathcal{G}}(\partial S) \leq \beta^* \text{Vol}_{\mathcal{H}}(\partial S), \quad \text{Vol}_{\mathcal{H}}(S) \leq \text{Vol}_{\mathcal{G}}(S) \leq \beta^* \text{Vol}_{\mathcal{H}}(S), \tag{7}$$

where $\beta^* = \max_{e \in E} \beta^{(e)}$. Applying spectral clustering on $\mathcal{G} = (V, E_o, w)$ produces the desired partition $(S^*, \bar{S}^*)$. The next result is a consequence of combining the bounds of (7) with the approximation guarantees of spectral graph clustering (Theorem 1 [15]).

3

Theorem 3.1. If the optimization problem (5) is feasible for all InH-hyperedges and the weights $w_{v\tilde{v}}$ obtained from (6) are nonnegative for all $\{v, \tilde{v}\} \in E_o$, then $\alpha^* = \text{NCut}_{\mathcal{H}}(S^*)$ satisfies

$$(\beta^*)^3 \alpha_{\mathcal{H}} \geq \frac{(\alpha^*)^2}{8} \geq \frac{\alpha_{\mathcal{H}}^2}{8}. \tag{8}$$

where $\alpha_{\mathcal{H}}$ is the optimal value of normalized cut of the hypergraph $\mathcal{H}$.

There are no guarantees that the $w_{v\tilde{v}}$ will be nonnegative: The optimization problem (5) may result in solutions $w^{(e)}$ that are negative. The performance of spectral methods in the presence of negative edge weights is not well understood [17, 18]; hence, it would be desirable to have the weights $w_{v\tilde{v}}$ generated from (6) be nonnegative. Unfortunately, imposing nonngativity constraints in the optimization problem may render it infeasible. In practice, one may use $(w_{v\tilde{v}})_+ = \max\{w_{v\tilde{v}}, 0\}$ to remove negative weights (other choices, such as $(w_{v\tilde{v}})_+ = \sum_e (w_{v\tilde{v}}^{(e)})_+$ do not appear to perform well). This change invalidates the theoretical result of Theorem 3.1, but provides solutions with very good empirical performance. The issues discussed are illustrated by the next example.

Example 3.1. Let $e = \{1, 2, 3\}$, $(w_e(\{1\}), w_e(\{2\}), w_e(\{3\})) = (0, 0, 1)$. The solution to the weight optimization problem is $(\beta^{(e)}, w_{12}^{(e)}, w_{13}^{(e)}, w_{23}^{(e)}) = (1, -1/2, 1/2, 1/2)$. If all components $w^{(e)}$ are constrained to be nonnegative, the optimization problem is infeasible. Nevertheless, the above choice of weights is very unlikely to be encountered in practice, as $w_e(\{1\}), w_e(\{2\}) = 0$ indicates that vertices 1 and 2 have no relevant connections within the given hyperedge e, while $w_e(\{3\}) = 1$ indicates that vertex 3 is strongly connected to 1 and 2, which is a contradiction. Let us assume next that the negative weight is set to zero. Then, we adjust the weights $((w_{12}^{(e)})_+, w_{13}^{(e)}, w_{23}^{(e)}) = (0, 1/2, 1/2)$, which produce clusterings ((1,3)(2)) or ((2,3)(1)); both have zero costs based on w_e.

Another problem is that arbitrary choices for w_e may cause the optimization problem to be infeasible (5) even if negative weights of $w^{(e)}$ are allowed, as illustrated by the following example.

Example 3.2. Let $e = \{1, 2, 3, 4\}$, with $w_e(\{1, 4\}) = w_e(\{2, 3\}) = 1$ and $w_e(S) = 0$ for all other choices of sets S. To force the weights to zero, we require $w_{v\tilde{v}}^{(e)} = 0$ for all pairs $v\tilde{v}$, which fails to work for $w_e(\{1, 4\}), w_e(\{2, 3\})$. For a hyperedge e, the degrees of freedom for w_e are $2^{\delta(e)-1} - 1$, as two values of w_e are fixed, while the other values are paired up by symmetry. When $\delta(e) > 3$, we have $\binom{\delta(e)}{2} < 2^{\delta(e)-1} - 1$, which indicates that the problem is overdetermined/infeasible.

In what follows, we provide sufficient conditions for the optimization problem to have a feasible solution with nonnegative values of the weights $w^{(e)}$. Also, we provide conditions for the weights w_e that result in a small constant β^* and hence allow for quadratic approximations of the optimum solution. Our results depend on the availability of information about the weights w_e: In practice, the weights have to be inferred from observable data, which may not suffice to determine more than the weight of singletons or pairs of elements.

Only the values of $w_e(\{v\})$ are known. In this setting, we are only given information about how much each node contributes to a higher-order relation, i.e., we are only given the values of $w_e(\{v\})$, $v \in V$. Hence, we have $\delta(e)$ costs (equations) and $\delta(e) \geq 2$ variables, which makes the problem underdetermined and easy to solve. The optimal $\beta^e = 1$ is attained by setting for all edges $\{v, \tilde{v}\}$

$$w_{v\tilde{v}}^{(e)} = \frac{1}{\delta(e) - 2} [w_e(\{v\}) + w_e(\{\tilde{v}\})] - \frac{1}{(\delta(e) - 1)(\delta(e) - 2)} \sum_{v' \in e} w_e(\{v'\}). \tag{9}$$

The components of $w_e(\cdot)$ with positive coefficients in (3) are precisely those associated with the endpoints of edges $v\tilde{v}$. Using simple algebraic manipulations, one can derive the conditions under which the values $w_{v\tilde{v}}^{(e)}$ are nonnegative, and these are presented in the Supplementary Material.

The solution to (9) produces a perfect projection with $\beta^{(e)} = 1$. Unfortunately, one cannot guarantee that the solution is nonnegative. Hence, the question of interest is to determine for what types of cuts can one can deviate from a perfect projection but ensure that the weights are nonnegative. The proposed approach is to set the unspecified values of $w_e(\cdot)$ so that the weight function becomes submodular, which guarantees nonnegative weights $w_{v\tilde{v}}^e$ that can constantly approximate $w_e(\cdot)$, although with a larger approximation constant β.

Submodular weights $w_e(S)$. As previously discussed, when $\delta(e) > 3$, the optimization problem (5) may not have any feasible solutions for arbitrary choices of weights. However, we show next that if

the weights w_e are *submodular*, then (5) always has a nonnegative solution. We start by recalling the definition of a submodular function.

Definition 3.2. A function $w_e : 2^e \to \mathbb{R}_{\geq 0}$ that satisfies

$$w_e(S_1) + w_e(S_2) \geq w_e(S_1 \cap S_2) + w_e(S_1 \cup S_2) \quad \text{for all } S_1, S_2 \in 2^e,$$

is termed submodular.

Theorem 3.3. If w_e is submodular, then

$$w_{v\tilde{v}}^{*(e)} = \sum_{S \in 2^e / \{\emptyset, e\}} \left[\frac{w_e(S)}{2|S|(\delta(e) - |S|)} 1_{|\{v, \tilde{v}\} \cap S| = 1} \right. \tag{10}$$

$$\left. - \frac{w_e(S)}{2(|S| + 1)(\delta(e) - |S| - 1)} 1_{|\{v, \tilde{v}\} \cap S| = 0} - \frac{w_e(S)}{2(|S| - 1)(\delta(e) - |S| + 1)} 1_{|\{v, \tilde{v}\} \cap S| = 2} \right]$$

is nonnegative. For $2 \leq \delta(e) \leq 7$, the function above is a feasible solution for the optimization problem (5) with parameters $\beta^{(e)}$ listed in Table 1.

Table 1: Feasible values of $\beta^{(e)}$ for $\delta^{(e)}$

$|\delta(e)|$	2	3	4	5	6	7
β	1	1	3/2	2	4	6

Theorem 3.3 also holds when some weights within w_e are not specified, but may be completed to satisfy submodularity constraints (See Example 3.3). Also, (10) lead to an optimal approximation ratio $\beta^{(e)}$ if we restrict $w^{(e)}$ to be a linear mapping of w_e, which is formally stated next.

Theorem 3.4. Suppose that for all pairs of $\{v, \tilde{v}\} \in E_o$, $w_{v\tilde{v}}^{(e)}$ is a linear function of w_e, denoted by $w_{v\tilde{v}}^{(e)} = f_{v\tilde{v}}(w_e)$, where $\{f_{v\tilde{v}}\}_{\{v\tilde{v} \in E^{(e)}\}}$ depends on $\delta(e)$ but not on w_e. Then, when $\delta(e) \leq 7$, the optimal values of β for the following optimization problem depend only on $\delta(e)$, and are equal to those listed in Table 1.

$$\min_{\{f_{v\tilde{v}}\}_{\{v, \tilde{v}\} \in E_o}} \quad \max_{\text{submodular } w_e} \quad \beta \tag{11}$$

$$\text{s.t.} \quad w_e(S) \leq \sum_{v \in S, \tilde{v} \in e/S} f_{v\tilde{v}}(w_e) \leq \beta w_e(S), \quad \text{for all } S \in 2^e.$$

Remark 3.1. Although we were able to prove feasibility (Theorem 3.3) and optimality of linear solutions (Theorem 3.4) only for small values of $\delta(e)$, we conjecture the results to be true for all $\delta(e)$.

Example 3.3. Let $e = \{1, 2, 3, 4\}$, $(w_e(\{1\}), w_e(\{2\}), w_e(\{3\}), w_e(\{4\})) = (1/3, 1/3, 1, 1)$. Solving (9) yields $w_{12}^{(e)} = -1/9$ and $\beta^{(e)} = 1$. By completing the missing components in w_e as $(w_e(\{1, 2\}), w_e(\{1, 3\}), w_e(\{1, 4\})) = (2/3, 1, 1)$ leads to submodular weights (Observe that completions are not necessarily unique). Then, the solution of (10) gives $w_{12}^{(e)} = 0$ and $\beta^{(e)} \in (1, 2/3]$, which is clearly larger than one.

4 Related Work and Discussion

One contribution of our work is to introduce the notion of an inhomogenous partition of hyperedges and a new hypergraph projection method that accompanies the procedure. Subsequent edge weight merging and spectral clustering are standardly used in hypergraph clustering algorithms, and in particular in Zhou's normalized hypergraph cut approach [13], Clique Expansion, Star Expansion and Clique Averaging [11]. The formulation closest to ours is Zhou's method [13]. In the aforementioned hypergraph clustering method for H-hyperedges, each hyperedge e is assigned a scalar weight w_e^{H}. For the projection step, Zhou used $w_e^{\text{H}}/\delta(e)$ for the weight of each pair of endpoints of e. If we view the H-hyperedge as an InH-hyperedge with weight function w_e, where $w_e(S) = w_e^{\text{H}}|S|(\delta(e) - |S|)/\delta(e)$ for all $S \in 2^e$, then our definition of the volume/cost of the boundary (2) is identical to that of Zhou's. With this choice of w_e, the optimization problem (5) outputs $w_{v\tilde{v}}^{(e)} = w_e^{\text{H}}/\delta(e)$, with $\beta^{(e)} = 1$, which are the same values as those obtained via Zhou's projection. The degree of a vertex

in [13] is defined as $d_v = \sum_{e \in E} h(e,v) w_e^{\mathrm{H}} = \sum_{e \in E} \frac{\delta(e)}{\delta(e)-1} w_e(\{v\})$, which is a weighted sum of the $w_e(\{v\})$ and thus takes a slightly different form when compared to our definition. As a matter of fact, for uniform hypergraphs, the two forms are same. Some other hypergraph clustering algorithms, such as Clique expansion and Star expansion, as shown by Agarwal et al. [19], represent special cases of our method for uniform hypergraphs as well.

The Clique Averaging method differs substantially from all the aforedescribed methods. Instead of projecting each hyperedge onto a subgraph and then combining the subgraphs into a graph, the algorithm performs a one-shot projection of the whole hypergraph onto a graph. The projection is based on a ℓ_2-minimization rule, which may not allow for constant-approximation solutions. It is unknown if the result of the procedure can provide a quadratic approximation for the optimum solution. Clique Averaging also has practical implementation problems and high computational complexity, as it is necessary to solve a linear regression with n^2 variable and $n^{\delta(e)}$ observations.

In the recent work on network motif clustering [10], the hyperedges are deduced from a graph where they represent so called motifs. Benson et. al [10] proved that if the motifs have three vertices, resulting in a three-uniform hypergraph, their proposed algorithm satisfies the Cheeger inequality for motifs[1]. In the described formulation, when cutting a H-hyperedge with weight w_e^{H}, one is required to pay w_e^{H}. Hence, recasting this model within our setting, we arrive at inhomogenous weights $w_e(S) = w_e^{\mathrm{H}}$, for all $S \in 2^e$, for which (5) yields $w_{v\tilde{v}}^{(e)} = w_e^{\mathrm{H}}/(\delta(e)-1)$ and $\beta^{(e)} = \lfloor \frac{\delta^2(e)}{4} \rfloor/(\delta(e)-1)$, identical to the solution of [10]. Furthermore, given the result of our Theorem 3.1, one can prove that the algorithm of [10] offers a quadratic-factor approximation for motifs involving more than three vertices, a fact that was not established in the original work [10].

5 Applications

Network motif clustering. Real-world networks exhibit rich higher-order connectivity patterns frequently referred to as network motifs [20]. Motifs are special subgraphs of the graph and may be viewed as hyperedges of a hypergraph over the same set of vertices. Recent work has shown that hypergraph clustering based on motifs may be used to learn hidden high-order organization patterns in networks [10, 8, 21]. However, this approach treats all vertices and edges within the motifs in the same manner, and hence ignores the fact that each structural unit within the motif may have a different relevance or different role. As a result, the vertices of the motifs are partitioned with a uniform cost. However, this assumption is hardly realistic as in many real networks, only some vertices of higher-order structures may need to be clustered together. Hence, inhomogenous hyperedges are expected to elucidate more subtle high-order organizations of network. We illustrate the utility of InH-partition on the Florida Bay foodweb [22] and compare our findings to those of [10].

The Florida Bay foodweb comprises 128 vertices corresponding to different species or organisms that live in the Bay, and 2106 directed edges indicating carbon exchange between two species. The Foodweb essentially represents a layered flow network, as carbon flows from so called producers organisms to high-level predators. Each layer of the network consists of "similar" species that play the same role in the food chain. Clustering of the species may be performed by leveraging the layered structure of the interactions. As a network motif, we use a subgraph of four species, and correspondingly, four vertices denoted by v_i, for $i = 1, 2, 3, 4$. The motif captures, among others, relations between two producers and two consumers: The producers v_1 and v_2 both transmit carbons to v_3 and v_4, and all types of carbon flow between v_1 and v_2, v_3 and v_4 are allowed (see Figure 2 Left). Such a motif is the smallest structural unit that captures the fact that carbon exchange occurs in uni-direction between layers, while is allowed freely within layers. The inhomogeneous hyperedge costs are assigned according to the following heuristics: First, as v_1 and v_2 share two common carbon recipients (predators) while v_3 and v_4 share two common carbon sources (preys), we set $w_e(\{v_i\}) = 1$ for $i = 1, 2, 3, 4$, and $w_e(\{v_1, v_2\}) = 0$, $w_e(\{v_1, v_3\}) = 2$, and $w_e(\{v_1, v_4\}) = 2$. Based on the solution of the optimization problem (5), one can construct a weighted subgraph whose costs of cuts match the inhomogeneous costs, with $\beta^{(e)} = 1$. The graph is depicted in Figure 2 (left).

Our approach is to perform hierarchical clustering via iterative application of the InH-partition method. In each iteration, we construct a hypergraph by replacing the chosen motif subnetwork by an hyperedge. The result is shown in Figure 2. At the first level, we partitioned the species into three

---

[1]The Cheeger inequality [15] arises in the context of minimizing the conductance of a graph, which is related to the normalized cut.
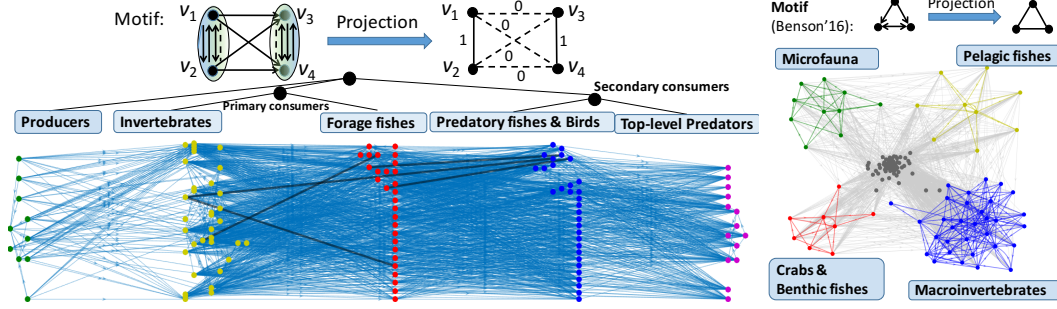
Figure 2: Motif clustering in the Florida Bay food web. Left: InHomogenous case. Left-top: Hyperedge (network motif) & the weighted induced subgraph; Left-bottom: Hierarchical clustering structure and five clusters via InH-partition. The vertices belonging to different clusters are distinguished by the colors of vertices. Edges with a uni-direction (right to left) are colored black while other edges are kept blue. Right: Homogenous partitioning [10] with four clusters. Grey vertices are not connected by motifs and thus unclassified.

clusters corresponding to producers, primary consumers and secondary consumers. The producer cluster is homogeneous in so far that it contains only producers, a total of nine of them. At the second level, we partitioned the obtained primary-consumer cluster into two clusters, one of which almost exclusively comprises invertebrates (28 out of 35), while the other almost exclusively comprises forage fishes. The secondary-consumer cluster is partitioned into two clusters, one of which comprises top-level predators, while the other cluster mostly consists of predatory fishes and birds. Overall, we recovered five clusters that fit five layers ranging from producers to top-level consumers. It is easy to check that the producer, invertebrate and top-level predator clusters exhibit high functional similarity of species ($> 80\%$). An exact functional classification of forage and predatory fishes is not known, but our layered network appears to capture an overwhelmingly large number of prey-predator relations among these species. Among the 1714 edges, obtained after removing isolated vertices and detritus species vertices, only five edges point in the opposite direction from a higher to a lower-level cluster, two of which go from predatory fishes to forage fishes. Detailed information about the species and clusters is provided in the Supplementary Material.

In comparison, the related work of Benson et al. [10] which used homogenous hypergraph clustering and triangular motifs reported a very different clustering structure. The corresponding clusters covered less than half of the species (62 out of 128) as many vertices were not connected by the triangle motif; in contrast, 127 out of 128 vertices were covered by our choice of motif. We attribute the shortcomings of the approach in [10] to a) the choice of the triangle network motif, which fails to connect all vertices unlike our "fan" motif that connects many vertices and promotes layered structures; b) the lack of inhomogeneous weights, as homogeneous weights produce only a giant cluster. Another orthogonal line of work used topological sorting to rank species based on their carbon flows [23]. Topological sorting cannot use biological side information and hence fails to automatically determine the boundaries of the clusters.

Learning the Riffled Independence Structure of Ranking Data. Learning probabilistic models for ranking data has attracted significant interest in social and political sciences as well as in machine learning [24, 25]. Recently, a probabilistic model, termed the riffled-independence model, was shown to accurately describe many benchmark ranked datasets [26]. In the riffled independence model, one first generates two rankings over two disjoint sets of element independently, and then riffle shuffles the rankings to arrive at an interleaved order. The structure learning problem in this setting reduces to distinguishing the two categories of elements based on limited ranking data. More precisely, let Q be the set of candidates to be ranked, with $|Q| = n$. A full ranking is a bijection $\sigma : Q \to [n]$, and for an $a \in Q$, $\sigma(a)$ denotes the position of candidate a in the ranking σ. We use $\sigma(a) < (>)\sigma(b)$ to indicate that a is ranked higher (lower) than b in σ. If $S \subseteq Q$, we use $\sigma_S : S \to [|S|]$ to denote the ranking σ projected onto the set S. We also use $S(\sigma) \triangleq \{\sigma(a) | a \in S\}$ to denote the subset of positions of elements in S. Let $\mathbb{P}(E)$ denote the probability of the event E. Riffled independence asserts that there exists a riffled-independent set $S \subset Q$, such that for a fixed ranking σ' over $[n]$,
$$\mathbb{P}(\sigma = \sigma') = \mathbb{P}(\sigma_S = \sigma'_S)\mathbb{P}(\sigma_{Q/S} = \sigma'_{Q/S})\mathbb{P}(S(\sigma) = S(\sigma')).$$

Suppose that we are given a set of rankings $\Sigma = \{\sigma^{(1)}, \sigma^{(2)}, ..., \sigma^{(m)}\}$ drawn independently according to some probability distribution $\mathbb{P}$. If $\mathbb{P}$ has a riffled-independent set S^*, the structure learning problem

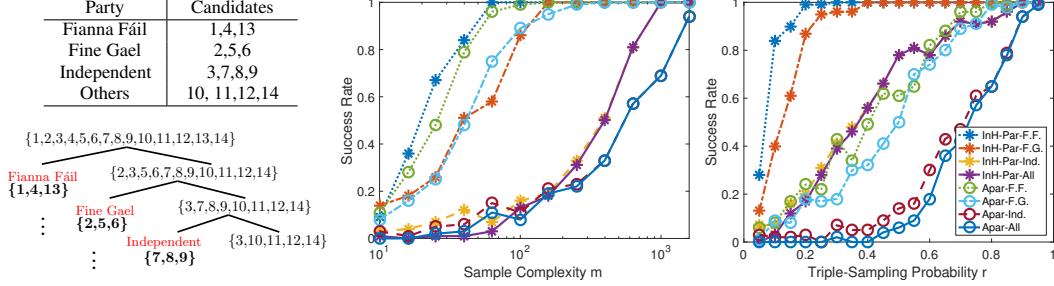| Party	Candidates
Fianna Fáil	1,4,13
Fine Gael	2,5,6
Independent	3,7,8,9
Others	10, 11,12,14

Figure 3: Election dataset. Left-top: parties and candidates; Left-bottom: hierarchical partitioning structure of Irish election detected by InH-Par; Middle: Success rate vs Sample Complexity; Right: Success rate vs Triple-sampling Rate.

is to find S^*. In [26], the described problem was cast as an optimization problem over all possible subsets of Q, with the objective of minimizing the Kullback-Leibler divergence between the ranking distribution with riffled independence and the empirical distribution of Σ [26]. A simplified version of the optimization problem reads as

$$\arg \min_{S \subset Q} \mathcal{F}(S) \triangleq \sum_{(i,j,k) \in \Omega^{cross}_{S,\bar{S}}} I_{i;j,k} + \sum_{(i,j,k) \in \Omega^{cross}_{\bar{S},S}} I_{i;j,k}, \quad (12)$$

where $\Omega^{cross}_{A,B} \triangleq \{(i,j,k)|i \in A, j, k \in B\}$, and where $I_{i;j,k}$ denotes the estimated mutual information between the position of the candidate i and two "comparison candidates" j, k. If $1_{\sigma(j)<\sigma(k)}$ indicates the indicator function of the underlying event, we may write

$$I_{i;j,k} \triangleq \hat{I}(\sigma(i); 1_{\sigma(j)<\sigma(k)}) = \sum_{\sigma(i)} \sum_{1_{\sigma(j)<\sigma(k)}} \hat{\mathbb{P}}(\sigma(i), 1_{\sigma(j)<\sigma(k)}) \log \frac{\hat{\mathbb{P}}(\sigma(i), 1_{\sigma(j)<\sigma(k)})}{\hat{\mathbb{P}}(\sigma(i))\mathbb{P}(1_{\sigma(j)<\sigma(k)})}, \quad (13)$$

where $\hat{\mathbb{P}}$ denotes an estimate of the underlying probability. If i and j, k are in different riffled-independent sets, the estimated mutual information $\hat{I}(\sigma(i); 1_{\sigma(j)<\sigma(k)})$ converges to zero as the number of samples increases.

One may recast the above problem as an InH-partition problem over a hypergraph where each candidate represents a vertex in the hypergraph, and $I_{i;j,k}$ represents the inhomogeneous cost $w_e(\{i\})$ for the hyperedge $e = \{i, j, k\}$; the optimization problem reduces to $\min_S \text{vol}_{\mathcal{H}}(\partial S)$. The two optimization tasks are different, and we illustrate next that the InH-partition outperforms the original optimization approach AnchorsPartition (Apar) [26] both on synthetic data and real data. Due to space limitations, synthetic data and a subset of the real dataset results are listed in the Supplementary Material.

Here, we analyzed the Irish House of Parliament election dataset (2002) [27]. The dataset consists of 2490 ballots fully ranking 14 candidates. The candidates were from a number of parties, where Fianna Fáil (F.F.) and Fine Gael (F.G.) are the two largest (and rival) Irish political parties. Using InH-partition (InH-Par), one can split the candidates iteratively into two sets (See Figure 3) which yields to meaningful clusters that correspond to large parties: $\{1, 4, 13\}$ (F.F.), $\{2, 5, 6\}$ (F.G.), $\{7, 8, 9\}$ (Ind.). We compared InH-partition with Apar based on their performance in detecting these three clusters using a small training set: We independently sampled m rankings 100 times and executed both algorithms to partition the set of candidates iteratively. During the partitioning procedure, "party success" was declared if one exactly detected one of the three party clusters ("F.F.", "F.G." & "Ind."). "All" was used to designate that all three party clusters were detected completely correctly. InH-partition outperforms Apar in recovering the clusters F.F. and Ind. and achieved comparable performance for cluster F.G.; hence, InH-partition offers superior overall performance compared to Apar. We also compared InH-partition with APar in the large sample regime ($m = 2490$), using only a subset of triple comparisons (hyperedges) sampled independently with probability r (This strategy significantly reduces the complexity of both algorithms). The average is computed over 100 independent runs. The results are shown in Figure 3, highlighting the robustness of InH-partition with respect to missing triples. Additional test on ranking data are described in the Supplementary Material, along with new results on subspace clustering, motion segmentation and others.

8

References

[1] A. K. Jain, M. N. Murty, and P. J. Flynn, "Data clustering: a review," *ACM computing surveys (CSUR)*, vol. 31, no. 3, pp. 264–323, 1999.

[2] A. Y. Ng, M. I. Jordan, and Y. Weiss, "On spectral clustering: Analysis and an algorithm," in *Advances in neural information processing systems*, 2002, pp. 849–856.

[3] S. R. Bulò and M. Pelillo, "A game-theoretic approach to hypergraph clustering," in *Advances in neural information processing systems*, 2009, pp. 1571–1579.

[4] M. Leordeanu and C. Sminchisescu, "Efficient hypergraph clustering." in *AISTATS*, 2012, pp. 676–684.

[5] H. Liu, L. J. Latecki, and S. Yan, "Robust clustering as ensembles of affinity relations," in *Advances in neural information processing systems*, 2010, pp. 1414–1422.

[6] N. Bansal, A. Blum, and S. Chawla, "Correlation clustering," in *Foundations of Computer Science, 2002. Proceedings. The 43rd Annual IEEE Symposium on*. IEEE, 2002, pp. 238–247.

[7] N. Ailon, M. Charikar, and A. Newman, "Aggregating inconsistent information: ranking and clustering," *Journal of the ACM (JACM)*, vol. 55, no. 5, p. 23, 2008.

[8] P. Li, H. Dau, G. Puleo, and O. Milenkovic, "Motif clustering and overlapping clustering for social network analysis," in *INFOCOM, 2017 Proceedings IEEE*. IEEE, 2017, pp. 109–117.

[9] S. Kim, S. Nowozin, P. Kohli, and C. D. Yoo, "Higher-order correlation clustering for image segmentation," in *Advances in neural information processing systems*, 2011, pp. 1530–1538.

[10] A. R. Benson, D. F. Gleich, and J. Leskovec, "Higher-order organization of complex networks," *Science*, vol. 353, no. 6295, pp. 163–166, 2016.

[11] S. Agarwal, J. Lim, L. Zelnik-Manor, P. Perona, D. Kriegman, and S. Belongie, "Beyond pairwise clustering," in *Computer Vision and Pattern Recognition, 2005. CVPR 2005. IEEE Computer Society Conference on*, vol. 2. IEEE, 2005, pp. 838–845.

[12] G. Chen and G. Lerman, "Spectral curvature clustering (scc)," *International Journal of Computer Vision*, vol. 81, no. 3, pp. 317–330, 2009.

[13] D. Zhou, J. Huang, and B. Schölkopf, "Learning with hypergraphs: Clustering, classification, and embedding," in *Advances in neural information processing systems*, 2007, pp. 1601–1608.

[14] H. Jeong, B. Tombor, R. Albert, Z. N. Oltvai, and A.-L. Barabási, "The large-scale organization of metabolic networks," *Nature*, vol. 407, no. 6804, pp. 651–654, 2000.

[15] F. R. Chung, "Four proofs for the cheeger inequality and graph partition algorithms," in *Proceedings of ICCM*, vol. 2, 2007, p. 378.

[16] J. Shi and J. Malik, "Normalized cuts and image segmentation," *IEEE Transactions on pattern analysis and machine intelligence*, vol. 22, no. 8, pp. 888–905, 2000.

[17] J. Kunegis, S. Schmidt, A. Lommatzsch, J. Lerner, E. W. De Luca, and S. Albayrak, "Spectral analysis of signed graphs for clustering, prediction and visualization," in *Proceedings of the 2010 SIAM International Conference on Data Mining*. SIAM, 2010, pp. 559–570.

[18] A. V. Knyazev, "Signed laplacian for spectral clustering revisited," *arXiv preprint arXiv:1701.01394*, 2017.

[19] S. Agarwal, K. Branson, and S. Belongie, "Higher order learning with graphs," in *Proceedings of the 23rd international conference on Machine learning*. ACM, 2006, pp. 17–24.

[20] R. Milo, S. Shen-Orr, S. Itzkovitz, N. Kashtan, D. Chklovskii, and U. Alon, "Network motifs: simple building blocks of complex networks," *Science*, vol. 298, no. 5594, pp. 824–827, 2002.

[21] C. Tsourakakis, J. Pachocki, and M. Mitzenmacher, "Scalable motif-aware graph clustering," *arXiv preprint arXiv:1606.06235*, 2016.

[22] "Florida bay trophic exchange matrix," http://vlado.fmf.uni-lj.si/pub/networks/data/bio/foodweb/Florida.paj.

[23] S. Allesina, A. Bodini, and C. Bondavalli, "Ecological subsystems via graph theory: the role of strongly connected components," *Oikos*, vol. 110, no. 1, pp. 164–176, 2005.

[24] P. Awasthi, A. Blum, O. Sheffet, and A. Vijayaraghavan, "Learning mixtures of ranking models," in *Advances in Neural Information Processing Systems*, 2014, pp. 2609–2617.

[25] C. Meek and M. Meila, "Recursive inversion models for permutations," in *Advances in Neural Information Processing Systems*, 2014, pp. 631–639.

[26] J. Huang, C. Guestrin *et al.*, "Uncovering the riffled independence structure of ranked data," *Electronic Journal of Statistics*, vol. 6, pp. 199–230, 2012.

[27] I. C. Gormley and T. B. Murphy, "A latent space model for rank data," in *Statistical Network Analysis: Models, Issues, and New Directions*. Springer, 2007, pp. 90–102.

[28] B. Bollobás, *Modern graph theory*. Springer Science & Business Media, 2013, vol. 184.

[29] R. L. Plackett, "The analysis of permutations," *Applied Statistics*, pp. 193–202, 1975.

[30] T. Kamishima, "Nantonac collaborative filtering: recommendation based on order responses," in *Proceedings of the ninth ACM SIGKDD international conference on Knowledge discovery and data mining*. ACM, 2003, pp. 583–588.

[31] R. Vidal, "Subspace clustering," *IEEE Signal Processing Magazine*, vol. 28, no. 2, pp. 52–68, 2011.

[32] J. P. Costeira and T. Kanade, "A multibody factorization method for independently moving objects," *International Journal of Computer Vision*, vol. 29, no. 3, pp. 159–179, 1998.

[33] R. Tron and R. Vidal, "A benchmark for the comparison of 3-d motion segmentation algorithms," in *Computer Vision and Pattern Recognition, 2007. CVPR'07. IEEE Conference on*. IEEE, 2007, pp. 1–8.

[34] R. Vidal, Y. Ma, and S. Sastry, "Generalized principal component analysis (gpca)," *IEEE Transactions on Pattern Analysis and Machine Intelligence*, vol. 27, no. 12, pp. 1945–1959, 2005.

[35] J. Yan and M. Pollefeys, "A general framework for motion segmentation: Independent, articulated, rigid, non-rigid, degenerate and non-degenerate," in *European conference on computer vision*. Springer, 2006, pp. 94–106.

[36] Y. Ma, H. Derksen, W. Hong, and J. Wright, "Segmentation of multivariate mixed data via lossy data coding and compression," *IEEE transactions on pattern analysis and machine intelligence*, vol. 29, no. 9, 2007.

[37] E. Elhamifar and R. Vidal, "Sparse subspace clustering," in *Computer Vision and Pattern Recognition, 2009. CVPR 2009. IEEE Conference on*. IEEE, 2009, pp. 2790–2797.

[38] P. Purkait, T.-J. Chin, A. Sadri, and D. Suter, "Clustering with hypergraphs: the case for large hyperedges," *IEEE Transactions on Pattern Analysis and Machine Intelligence*, 2016.

A Conductance of a Cut for an Inhomogeneous Hypergraph

The conductance of a cut $(S, \bar{S})$ for an inhomogeneous hypergraph is defined according to

$$\psi_{\mathcal{H}}(S) = \frac{\text{vol}_{\mathcal{H}}(\partial S)}{\min\{\text{vol}_{\mathcal{H}}(S), \text{vol}_{\mathcal{H}}(\bar{S})\}}. \tag{14}$$

This definition is consistent with the definition of conductance of a graph cut [28] and homogeneoous hypergraph cut [10]. The conductance is an upper bound for the normalized cut

$$\psi_{\mathcal{H}}(S) \geq \frac{1}{2}\text{NCut}_{\mathcal{H}}(S). \tag{15}$$

B A Brief Overview of Spectral Graph Partitioning

The combinatorial optimization problem of minimizing the NCut (3) for graphs is known to be NP-complete [16]. However, an efficient algorithm based on spectral techniques (Algorithm 1 below) can produce a solution within a quadratic factor of the optimum (Theorem. B.1).

Algorithm 1: Spectral Graph Partitioning
Input: The adjacency matrix A of the graph $\mathcal{G}$.
 Step 1: Construct the diagonal degree matrix D, with $D_{ii} = \sum_{j=1}^n A_{ij}$ for all $i \in [n]$.
 Step 2: Construct the normalized Laplacian matrix $\mathcal{L} = I - D^{-1/2}AD^{-1/2}$.
 Step 3: Compute the eigenvector $\mathbf{u} = (u_1, u_2, ..., u_n)^T$ corresponding to the second smallest eigenvalue of $\mathcal{L}$.
 Step 4: Let ℓ_i be the index of the i-th smallest entry of $D^{-1/2}\mathbf{u}$.
 Step 5: Compute $S = \arg\min_{S_i, 1 \leq i \leq n-1} \text{NCut}_{\mathcal{G}}(S_i)$ over all sets $S_i = \{\ell_1, \ell_2, \ldots, \ell_i\}$.
Output: Output S if $|S| < |\bar{S}|$, and $\bar{S}$ otherwise.

Theorem B.1. [**Derived based on Theorem 1 [15]**] Let α denote the value of the NCut output by Algorithm 1, and let $\alpha_{\mathcal{G}}$ denotes the optimal NCut of the graph $\mathcal{G}$. Also, let $\lambda_{\mathcal{G}}$ stand for the second smallest eigenvalue of normalized Laplacian matrix $\mathcal{L}$. Then,

$$\alpha_{\mathcal{G}} \geq \lambda_{\mathcal{G}} \geq \frac{\alpha^2}{8} \geq \frac{\alpha_{\mathcal{G}}^2}{8}. \tag{16}$$

Proof. Let S^* denote the output of Algorithm 1. We have $\alpha_{\mathcal{G}} \leq \text{NCut}_{\mathcal{G}}(S^*) = \alpha$ based on the definition of $\alpha_{\mathcal{G}}$. Suppose that $\alpha_{\mathcal{G}}$ is achieved by the set S_o, i.e., that

$$\alpha_{\mathcal{G}} = \text{vol}_{\mathcal{G}}(\partial S_o) \left(\frac{1}{\text{vol}_{\mathcal{G}}(S_o)} + \frac{1}{\text{vol}_{\mathcal{G}}(\bar{S}_o)} \right).$$

Let V be the vertices of $\mathcal{G}$. We define the following function g over V

$$g(v) = 1_{v \in S_o} - \frac{\text{vol}_{\mathcal{G}}(S_o)}{\text{vol}_{\mathcal{G}}(V)}, \quad \forall\, v \in V.$$

Recall that d_v is the degree of vertex v. It is easy to check that $\sum_{v \in V} g(v)d_v = 0$. Hence, due to the definition of $\lambda_{\mathcal{G}}$, we have

$$\lambda_{\mathcal{G}} \leq \frac{g^T(D - A)g}{g^T Dg} = \alpha_{\mathcal{G}},$$

where A denotes the adjacency matrix of the graph and D is a diagonal matrix whose diagonal entries equal to the degrees of the corresponding vertices. According to Theorem 1 [15] and the results of (15), we have

$$\lambda_{\mathcal{G}} \geq \frac{\psi_{\mathcal{G}}^2(S^*)}{2} \geq \frac{\alpha^2}{8},$$

which concludes the proof. □

For k-way partitions, Step 3 of the previously described algorithm entails computing the eigenvectors corresponds to the k smallest eigenvalues of $\mathcal{L}$. The i-th components of these k eigenvectors may be viewed as the coordinates of a representation for vertex v_i. Partitioning is performed by using the eigenvector representations of the vertices in some distance-based clustering algorithms, such as k-means.

C   Proof of Theorem 3.1

Assume that the optimization problem (5) is feasible for all InH-hyperedges, and recall that $\beta^* = \max_{e \in E} \beta^{(e)}$. Then $\mathcal{G} = (V, E_o, w)$ can constantly approximate the original hypergraph $\mathcal{H}$ in the sense that

$$\mathrm{Vol}_{\mathcal{H}}(\partial S) \leq \mathrm{Vol}_{\mathcal{G}}(\partial S) \leq \beta^* \mathrm{Vol}_{\mathcal{H}}(\partial S), \quad \mathrm{Vol}_{\mathcal{H}}(S) \leq \mathrm{Vol}_{\mathcal{G}}(S) \leq \beta^* \mathrm{Vol}_{\mathcal{H}}(S). \qquad (17)$$

Furthermore, recall that $w_{v\tilde{v}}$ is the weight of the edge $v\tilde{v}$ of the graph $\mathcal{G}$. If the weights $w_{v\tilde{v}}$ are non-negative for all $\{v, \tilde{v}\} \in E_o$, we can use Theorem B.1 when performing Algorithm 1 over the graph $\mathcal{G}$. Combining Theorem B.1 and equation (17), we have

$$(\beta^*)^3 \alpha_{\mathcal{H}} \geq \frac{(\alpha^*)^2}{8} \geq \frac{\alpha_{\mathcal{H}}^2}{8}, \qquad (18)$$

which concludes the proof.

D   Proof of Theorem 3.3

First, recall that $w_{v\tilde{v}}^{*(e)}$ denotes the projection weight of equation (10), for the case that $w_e(\cdot)$ is submodular:

$$w_{v\tilde{v}}^{*(e)} = \sum_{S \in 2^e / \{\emptyset, e\}} \left[\frac{w_e(S)}{2|S|(\delta(e) - |S|)} 1_{|\{v, \tilde{v}\} \cap S| = 1} \qquad (19) \right.$$

$$\left. - \frac{w_e(S)}{2(|S| + 1)(\delta(e) - |S| - 1)} 1_{|\{v, \tilde{v}\} \cap S| = 0} - \frac{w_e(S)}{2(|S| - 1)(\delta(e) - |S| + 1)} 1_{|\{v, \tilde{v}\} \cap S| = 2} \right]$$

We start by proving that for a fixed pair of vertices v and $\tilde{v}$, the weights $w_{v\tilde{v}}^{*(e)}$ are nonnegative provided that the $w_e(\cdot)$ are submodular. Note that the sum on the right-hand side of (19) is over all proper subsets S. The coefficients of $w_e(S)$ are positive if and only if S contains exactly one of the endpoints v and $\tilde{v}$. The idea behind the proof is to construct bijections between the subsets with positive coefficients and those with negative coefficients and cancel negative and positive terms.

We partition the power set 2^e into four parts, namely

$$\mathbb{S}_1 \triangleq \{S \in 2^e : v \in S, \tilde{v} \notin S\},$$
$$\mathbb{S}_2 \triangleq \{S \in 2^e : v \notin S, \tilde{v} \in S\},$$
$$\mathbb{S}_3 \triangleq \{S \in 2^e : v \notin S, \tilde{v} \notin S\},$$
$$\mathbb{S}_4 \triangleq \{S \in 2^e : v \in S, \tilde{v} \in S\}.$$

Choose any $S_1 \in \mathbb{S}_1$ and construct the unique sets $S_2 = S_1 / \{v\} \cup \{\tilde{v}\} \in \mathbb{S}_2$, $S_3 = S_1 / \{v\} \in \mathbb{S}_3$, $S_4 = S_1 \cup \{\tilde{v}\} \in \mathbb{S}_4$. Consequently, each set may be reconstructed from another set in the group, and we denote this set of bijective relations by $S_1 \leftrightarrow S_2 \leftrightarrow S_3 \leftrightarrow S_4$. Let $s = |S_1|$. Due to the way the sets S_1 and S_2 are chosen, the corresponding coefficients of $w_e(S_1)$ and $w_e(S_2)$ in (10) are both equal to

$$\frac{1}{2s(\delta(e) - s)}.$$

We also observe that the corresponding coefficients of $w_e(S_3)$ and $w_e(S_4)$ are

$$-\frac{1}{2s(\delta(e) - s)}.$$

Note that the submodularity property

$$w_e(S_1) + w_e(S_2) \geq w_e(S_3) + w_e(S_4),$$

allows us to cancel out the negative terms in the sum (19). This proves the claimed result.

Next, we prove that the optimization problem (5) has a feasible solution.

Recall that $G_e = (V^{(e)}, E^{(e)}, w^{(e)})$ is the subgraph obtained by projecting e. Set $w^{(e)} = w^{*(e)}$. For simplicity of notation, we denote the volume of the boundary of S over G_e as

$$\text{Vol}_{G_e}(\partial S) = \sum_{v \in S, \tilde{v} \in e/S} w_{v\tilde{v}}^{(e)}, \qquad \text{for } S \in 2^e.$$

The existence of a feasible solution of the optimization problem may be verified by checking that for any $S \in 2^e/\{\emptyset, e\}$, and for a given $\beta^{(e)}$, we have the following bounds on the volume of the boundary of S:

$$w_e(S) \leq \text{Vol}_{G_e}(\partial S) \leq \beta^{(e)} w_e(S).$$

Due to symmetry, we only need to perform the verification for sets S of different cardinalities $|S| \leq \delta(e)/2$. This verification is performed on a case-by-case bases, as we could not establish a general proof for arbitrary degree $\delta(e) \geq 2$. In what follows, we show that the claim holds true for all $\delta(e) \leq 7$; based on several special cases considered, we conjecture that the result is also true for all values of $\delta(e)$ greater than seven.

For notational simplicity, we henceforth assume that the vertices in e are labeled by elements in $\{1, 2, 3, ..., \delta(e)\}$.

First, note that by combining symmetry and submodularity, we can easily show that

$$w_e(S_1) + w_e(S_2) = w_e(S_1) + w_e(\bar{S}_2) \geq w_e(S_1 \cup \bar{S}_2) + w_e(S_1 \cap \bar{S}_2) = w_e(S_2/S_1) + w_e(S_1/S_2).$$

We iteratively use this equality in our subsequent proofs, following a specific notational format for all relevant inequalities:

$$v_{i_1}, ..., v_{i_r} \in S_1, \ v_{j_1}, ..., v_{j_s} \in S_2, \ \textit{Weight inequality} \implies \textit{Volume inequality}.$$

The above line asserts that for all ordered subsets $(v_{i_1}, ..., v_{i_r})$ and $(v_{j_1}, ..., v_{j_s})$ chosen from S_1 and S_2 without replacement, respectively, we have that the *Weight inequalities* follow based on the properties of $w_e(\cdot)$. These *Weight inequalities* are consequently inserted into the formula for the volume $\text{Vol}_{G_e}(S)$ to arrive at the *Volume inequality* for $\text{Vol}_{G_e}(S)$.

For $\delta(e) = 2$, the projection (19) is just a "self-projection": It is easy to check that for any singleton S, $\text{Vol}_{G_e}(\partial S) = w_e(S)$ and hence $\beta^{(e)} = 1$. We next establish the same claim for larger hyperedge sizes $\delta(e)$.

D.1 $\delta(e) = 3$, $\beta^{(e)} = 1$

By using the symmetry property of $w_e(\cdot)$ we have

$$w_{12}^{*(e)} = \frac{1}{2}(w_e(\{1\}) + w_e(\{2\})) - w_e(\{3\}).$$

Therefore, $\text{Vol}_{G_e}(\partial\{1\}) = w_{12}^{*(e)} + w_{13}^{*(e)} = w_e(\{1\})$ and hence $\beta^{(e)} = 1$.

D.2 $\delta(e) = 4$, $\beta^{(e)} = 3/2$

By using the symmetry property of $w_e(\cdot)$ we have

$$w_{12}^{*(e)}$$
$$= \frac{1}{3}(w_e(\{1\}) + w_e(\{2\})) - \frac{1}{4}(w_e(\{3\}) + w_e(\{4\}))$$
$$+ \frac{1}{4}w_e(\{1, 2\}) + w_e(\{1, 3\})) - \frac{1}{3}w_e(\{1, 4\}).$$

The basic idea behind the proof of the equalities to follow is to carefully select subsets for which the submodular inequality involving $w_e(\cdot)$ may be used to eliminate the terms corresponding to the volumes $\text{Vol}_{G_e}(\partial S)$.

13

Case $S = \{1\}$:

$$\mathrm{Vol}_{G_e}(\partial\{1\})$$

$$=w_e(\{1\}) - \frac{1}{6}(w_e(\{2\}) + w_e(\{3\}) + w_e(\{4\}))$$

$$+\frac{1}{6}(w_e(\{1,2\}) + w_e(\{1,3\}) + w_e(\{1,4\}))$$

$v_1 = 1, \; v_2, v_3 \in \{2,3,4\}, \; w_e(\{v_1, v_2\}) + w_e(\{v_1, v_3\}) \geq w_e(\{v_2\}) + w_e(\{v_3\})$
$$\implies \quad \mathrm{Vol}_{G_e}(\partial\{1\}) \geq w_e(\{1\}).$$

$v_1 = 1, \; v_2 \in \{2,3,4\}, \; w_e(\{v_1, v_2\}) \leq w_e(\{v_1\}) + w_e(\{v_2\})$
$$\implies \quad \mathrm{Vol}_{G_e}(\partial\{1\}) \leq \frac{3}{2}w_e(\{1\}).$$

Case $S = \{1,2\}$:

$$\mathrm{Vol}_{G_e}(\partial\{1,2\})$$

$$=\frac{1}{6}(w_e(\{1\}) + w_e(\{2\}) + w_e(\{3\}) + w_e(\{4\}))$$

$$+w_e(\{1,2\}) - \frac{1}{6}(w_e(\{1,3\}) + w_e(\{1,4\}))$$

$v_1 \in \{1,2\}, \; v_2 \in \{3,4\}, \; w_e(\{v_1\}) + w_e(\{v_2\}) \geq w_e(\{v_1, v_2\})$
$$\implies \quad \mathrm{Vol}_{G_e}(\partial\{1,2\}) \geq w_e(\{1,2\}).$$

$v_1, v_2 \in \{1,2\}, v_3 \in \{3,4\}, \; w_e(\{v_1\}) + w_e(\{v_3\}) \leq w_e(\{v_1, v_2\}) + w_e(\{v_2, v_3\})$
$$\implies \quad \mathrm{Vol}_{G_e}(\partial\{1,2\}) \leq \frac{4}{3}w_e(\{1,2\}).$$

D.3 $\delta(e) = 5, \; \beta^{(e)} = 2$

By using the symmetry property of $w_e(\cdot)$ we have

$$w_{12}^{*(e)}$$

$$=\frac{1}{4}(w_e(\{1\}) + w_e(\{2\})) - \frac{1}{6}(w_e(\{3\}) + w_e(\{4\}) + w_e(\{5\})) - \frac{1}{4}w_e(\{1,2\})$$

$$+\frac{1}{6}(w_e(\{1,3\}) + w_e(\{1,4\}) + w_e(\{1,5\}) + w_e(\{2,3\}) + w_e(\{2,4\}) + w_e(\{2,5\}))$$

$$-\frac{1}{6}(w_e(\{3,4\}) + w_e(\{3,5\}) + w_e(\{4,5\})).$$

Case $S = \{1\}$:

$$\mathrm{Vol}_{G_e}(\partial\{1\})$$

$$=w_e(\{1\}) - \frac{1}{4}(w_e(\{2\}) + w_e(\{3\}) + w_e(\{4\}) + w_e(\{5\}))$$

$$+\frac{1}{4}(w_e(\{1,2\}) + w_e(\{1,3\}) + w_e(\{1,4\}) + w_e(\{1,5\}))$$

$v_1 = 1, \; v_2, v_3 \in \{2,3,4,5\}, \; w_e(\{v_1, v_2\}) + w_e(\{v_1, v_3\}) \geq w_e(\{v_2\}) + w_e(\{v_3\})$
$$\implies \quad \mathrm{Vol}_{G_e}(\partial\{1\}) \geq w_e(\{1\}).$$

$v_1 = 1, \; v_2 \in \{2,3,4,5\}, \; w_e(\{v_1, v_2\}) \leq w_e(\{v_1\}) + w_e(\{v_2\})$
$$\implies \quad \mathrm{Vol}_{G_e}(\partial\{1\}) \leq 2w_e(\{1\}).$$

Case $S = \{1, 2\}$:

$$\text{Vol}_{G_e}(\partial\{1,2\})$$

$$=\frac{1}{4}(w_e(\{1\}) + w_e(\{2\})) - \frac{1}{6}(w_e(\{3\}) + w_e(\{4\}) + w_e(\{5\})) + w_e(\{1,2\})$$

$$-\frac{1}{12}(w_e(\{1,3\}) + w_e(\{1,4\}) + w_e(\{1,5\}) + w_e(\{2,3\}) + w_e(\{2,4\}) + w_e(\{2,5\}))$$

$$+\frac{1}{3}(w_e(\{3,4\}) + w_e(\{3,5\}) + w_e(\{4,5\}))$$

$v_1, v_2, v_3 \in \{3,4,5\}, \ w_e(\{v_2\}) + w_e(\{v_3\}) \leq w_e(\{v_1, v_2\}) + w_e(\{v_1, v_3\})$
$v_1 \in \{1,2\}, \ v_2 \in \{3,4,5\}, \ w_e(\{v_1, v_2\}) \leq w_e(\{v_1\}) + w_e(\{v_2\})$
$$\implies \quad \text{Vol}_{G_e}(\partial\{1,2\}) \geq w_e(\{1,2\}).$$

$v_1 \in \{1,2\}, \ v_2, v_3 \in \{3,4,5\}, \ w_e(\{v_1, v_2\}) + w_e(\{v_1, v_3\}) \geq w_e(\{v_2\}) + w_e(\{v_3\})$
$v_1, v_2 \in \{1,2\}, \ v_3, v_4, v_5 \in \{3,4,5\}, \ w_e(\{v_3, v_4\}) \leq w_e(\{v_1, v_2\}) + w_e(\{v_5\})$
$$\implies \quad \text{Vol}_{G_e}(\partial\{1,2\}) \leq 2w_e(\{1,2\}).$$

D.4 $\delta(e) = 6, \ \beta^{(e)} = 4$

By using the symmetry property of $w_e(\cdot)$ we have

$$w_{12}^{*(e)}$$

$$=\frac{1}{5}(w_e(\{1\}) + w_e(\{2\})) - \frac{1}{8}(w_e(\{3\}) + w_e(\{4\}) + w_e(\{5\}) + w_e(\{6\})) - \frac{1}{5}w_e(\{1,2\})$$

$$+\frac{1}{8}(w_e(\{1,3\}) + w_e(\{1,4\}) + w_e(\{1,5\}) + w_e(\{1,6\}) + w_e(\{2,3\}) + w_e(\{2,4\})$$

$$+ w_e(\{2,5\}) + w_e(\{2,6\}))$$

$$-\frac{1}{9}(w_e(\{3,4\}) + w_e(\{3,5\}) + w_e(\{3,6\}) + w_e(\{4,5\}) + w_e(\{4,6\}) + w_e(\{5,6\}))$$

$$-\frac{1}{9}(w_e(\{1,2,3\}) + w_e(\{1,2,4\}) + w_e(\{1,2,5\}) + w_e(\{1,2,6\}))$$

$$+\frac{1}{8}(w_e(\{1,3,4\}) + w_e(\{1,3,5\}) + w_e(\{1,3,6\}) + w_e(\{1,4,5\})$$

$$+ w_e(\{1,4,6\}) + w_e(\{1,5,6\}))$$

Case $S = \{1\}$:

$$\text{Vol}_{G_e}(\partial\{1\})$$

$$=w_e(\{1\}) - \frac{3}{10}(w_e(\{2\}) + w_e(\{3\}) + w_e(\{4\}) + w_e(\{5\}) + w_e(\{6\}))$$

$$+\frac{3}{10}(w_e(\{1,2\}) + w_e(\{1,3\}) + w_e(\{1,4\}) + w_e(\{1,5\}) + w_e(\{1,6\}))$$

$$-\frac{1}{12}(w_e(\{2,3\}) + w_e(\{2,4\}) + w_e(\{2,5\}) + w_e(\{2,6\}) + w_e(\{3,4\})$$

$$+ w_e(\{3,5\}) + w_e(\{3,6\}) + w_e(\{4,5\}) + w_e(\{4,6\}) + w_e(\{5,6\}))$$

$$+\frac{1}{12}(w_e(\{1,2,3\}) + w_e(\{1,2,4\}) + w_e(\{1,2,5\}) + w_e(\{1,2,6\})$$

$$+ w_e(\{1,3,4\}) + w_e(\{1,3,5\}) + w_e(\{1,3,6\})$$

$$+ w_e(\{1,4,5\}) + w_e(\{1,4,6\}) + w_e(\{1,5,6\}))$$

$$v_1 = 1, \ v_2, v_3 \in \{2,3,4,5,6\}, \ w_e(\{v_1, v_2\}) + w_e(\{v_1, v_3\}) \geq w_e(\{v_2\}) + w_e(\{v_3\})$$
$$v_1 = 1, \ v_2, v_3, v_4, v_5 \in \{2,3,4,5,6\},$$
$$w_e(\{v_1, v_2, v_3\}) + w_e(\{v_1, v_4, v_5\}) \geq w_e(\{v_2, v_3\}) + w_e(\{v_4, v_5\})$$
$$\implies \mathrm{Vol}_{G_e}(\partial\{1\}) \geq w_e(\{1\}).$$

$$v_1 = 1, \ v_2 \in \{2,3,4,5,6\}, \ w_e(\{v_1, v_2\}) \leq w_e(\{v_1\}) + w_e(\{v_2\})$$
$$v_1 = 1, \ v_2, v_3 \in \{2,3,4,5,6\}, \ w_e(\{v_1, v_2, v_3\}) \leq w_e(\{v_1\}) + w_e(\{v_2, v_3\})$$
$$\implies \quad \mathrm{Vol}_{G_e}(\partial\{1\}) \leq \frac{10}{3} w_e(\{1\}).$$

Case $S = \{1,2\}$:

$\mathrm{Vol}_{G_e}(\partial\{1,2\})$

$$= \frac{3}{10}(w_e(\{1\}) + w_e(\{2\})) - \frac{7}{20}(w_e(\{3\}) + w_e(\{4\}) + w_e(\{5\}) + w_e(\{6\}))$$

$$+ w_e(\{1,2\}) - \frac{1}{30}(w_e(\{1,3\}) + w_e(\{1,4\}) + w_e(\{1,5\}) + w_e(\{1,6\}) + w_e(\{2,3\})$$
$$+ w_e(\{2,4\}) + w_e(\{2,5\}) + w_e(\{2,6\}))$$

$$+ \frac{1}{18}(w_e(\{3,4\}) + w_e(\{3,5\}) + w_e(\{3,6\}) + w_e(\{4,5\}) + w_e(\{4,6\}) + w_e(\{5,6\}))$$

$$+ \frac{5}{12}(w_e(\{1,2,3\}) + w_e(\{1,2,4\}) + w_e(\{1,2,5\}) + w_e(\{1,2,6\}))$$

$$- \frac{1}{18}(w_e(\{1,3,4\}) + w_e(\{1,3,5\}) + w_e(\{1,3,6\}) + w_e(\{1,4,5\}) + w_e(\{1,4,6\}) + w_e(\{1,5,6\}))$$

$$v_1 \in \{1,2\}, \ v_2 \in \{3,4,5,6\}, \ w_e(\{v_1, v_2\}) \leq w_e(\{v_1\}) + w_e(\{v_2\})$$
$$v_1 = 1, \ v_2 = 2, \ v_3, v_4 \in \{3,4,5,6\}, \ w_e(\{v_3\}) + w_e(\{v_4\}) \leq w_e(\{v_1, v_2, v_3\}) + w_e(\{v_1, v_2, v_4\})$$
$$v_1 = 1, \ v_2, v_3 \in \{3,4,5,6\}, \ w_e(\{v_1, v_2, v_3\}) \leq w_e(\{v_1\}) + w_e(\{v_2, v_3\})$$
$$\implies \quad \mathrm{Vol}_{G_e}(\partial\{1,2\}) \geq w_e(\{1,2\}).$$

$$v_1 = 1, \ v_2 = 2, \ v_3 \in \{3,4,5,6\}, \ w_e(\{v_3\}) \geq w_e(\{v_1, v_2, v_3\}) - w_e(\{v_1, v_2\})$$
$$v_1, v_2 \in \{1,2\}, \ v_3 \in \{3,4,5,6\}, \ w_e(\{v_1, v_3\}) \geq w_e(\{v_1\}) + w_e(\{v_1, v_2, v_3\}) - w_e(\{v_1, v_2\})$$
$$v_1, v_2 \in \{1,2\}, \ v_3, v_4, v_5, v_6 \in \{3,4,5,6\}, \ w_e(\{v_1, v_3, v_4\}) \geq w_e(\{v_5, v_6\}) + w_e(\{v_1\}) - w_e(\{v_1, v_2\})$$
$$\implies \quad \mathrm{Vol}_{G_e}(\partial\{1,2\}) \leq 3 w_e(\{1,2\}).$$

Case $S = \{1,2,3\}$:

$\mathrm{Vol}_{G_e}(\partial\{1,2,3\})$

$$= -\frac{3}{20}(w_e(\{1\}) + w_e(\{2\}) + w_e(\{3\}) + w_e(\{4\}) + w_e(\{5\}) + w_e(\{6\}))$$

$$+ \frac{5}{12}(w_e(\{1,2\}) + w_e(\{1,3\}) + w_e(\{2,3\} + w_e(\{4,5\}) + w_e(\{4,6\}) + w_e(\{5,6\}))$$

$$- \frac{13}{90}(w_e(\{1,4\}) + w_e(\{1,5\}) + w_e(\{1,6\}) + w_e(\{2,4\}) + w_e(\{2,5\}) + w_e(\{2,6\})$$
$$+ w_e(\{3,4\}) + w_e(\{3,5\}) + w_e(\{3,6\}))$$

$$+ w_e(\{1,2,3\}) + \frac{1}{18}(w_e(\{1,2,4\}) + w_e(\{1,2,5\}) + w_e(\{1,2,6\}) + w_e(\{1,3,4\})$$
$$+ w_e(\{1,3,5\}) + w_e(\{1,3,6\}) + w_e(\{1,4,5\}) + w_e(\{1,4,6\}) + w_e(\{1,5,6\}))$$

$$v_1, v_2, v_3 \in \{1,2,3\}, \ v_4, v_5, v_6 \in \{4,5,6\}, \ w_e(\{v_2\}) + w_e(\{v_3\}) \leq w_e(\{v_1, v_2\}) + w_e(\{v_1, v_3\}),$$
$$w_e(\{v_5\}) + w_e(\{v_6\}) \leq w_e(\{v_4, v_5\}) + w_e(\{v_4, v_6\})$$
$$v_1, v_2, v_3 \in \{1,2,3\}, \ v_4, v_5, v_6 \in \{4,5,6\}, \ w_e(\{v_1, v_2\}) + w_e(\{v_4, v_5\}) \leq w_e(\{v_3, v_6\})$$
$$v_1, v_2, v_3 \in \{1,2,3\}, \ v_4, v_5, v_6 \in \{4,5,6\}, \ w_e(\{v_1, v_2, v_4\}) + w_e(\{v_1, v_4, v_5\}) \leq w_e(\{v_1, v_4\}) + w_e(\{v_3, v_6\})$$
$$\implies \quad \mathrm{Vol}_{G_e}(\partial\{1,2,3\}) \geq w_e(\{1,2,3\}).$$

16

$v_1, v_2 \in \{1,2,3\}, \; v_4, v_5 \in \{4,5,6\}, \; w_e(\{v_1, v_4, v_5\}) \leq w_e(\{v_1, v_4\}) + w_e(\{v_1, v_5\}) - w_e(\{v_1\}),$
$$w_e(\{v_1, v_2, v_4\}) \leq w_e(\{v_1, v_4\}) + w_e(\{v_2, v_4\}) - w_e(\{v_4\})$$
$v_1, v_2, v_3 \in \{1,2,3\}, \; v_4, v_5, v_6 \in \{4,5,6\}, \; w_e(\{v_1, v_4\}) \geq w_e(\{v_1\}) + w_e(\{v_5, v_6\}) - w_e(\{v_1, v_2, v_3\})$
$v_1, v_2, v_3 \in \{1,2,3\}, \; v_4, v_5, v_6 \in \{4,5,6\}, \; w_e(\{v_1\}) + w_e(\{v_2\}) \geq w_e(\{v_1, v_2\}),$
$$w_e(\{v_1\}) \geq w_e(\{v_2, v_3\}) - w_e(\{v_1, v_2, v_3\}),$$
$$w_e(\{v_4\}) + w_e(\{v_5\}) \geq w_e(\{v_4, v_5\}),$$
$$w_e(\{v_4\}) \geq w_e(\{v_5, v_6\}) - w_e(\{v_4, v_5, v_6\})$$
$$\implies \quad \text{Vol}_{G_e}(\partial\{1,2,3\}) \leq 4w_e(\{1,2,3\}).$$

D.5 $\delta(e) = 7$, $\beta^{(e)} = 6$

By using the symmetry property of $w_e(\cdot)$ we have

$w_{12}^{*(e)}$

$= \frac{1}{6}(w_e(\{1\}) + w_e(\{2\})) - \frac{1}{10}(w_e(\{3\}) + w_e(\{4\}) + w_e(\{5\}) + w_e(\{6\}) + w_e(\{7\}))$

$- \frac{1}{6}w_e(\{1,2\}) + \frac{1}{10}(w_e(\{1,3\}) + w_e(\{1,4\}) + w_e(\{1,5\}) + w_e(\{1,6\}) + w_e(\{1,7\})$

$\qquad + w_e(\{2,3\}) + w_e(\{2,4\}) + w_e(\{2,5\}) + w_e(\{2,6\}) + w_e(\{2,7\}))$

$- \frac{1}{12}(w_e(\{3,4\}) + w_e(\{3,5\}) + w_e(\{3,6\}) + w_e(\{3,7\}) + w_e(\{4,5\}) + w_e(\{4,6\})$

$\qquad + w_e(\{4,7\}) + w_e(\{5,6\}) + w_e(\{5,7\}) + w_e(\{6,7\}))$

$- \frac{1}{10}(w_e(\{1,2,3\}) + w_e(\{1,2,4\}) + w_e(\{1,2,5\}) + w_e(\{1,2,6\}) + w_e(\{1,2,7\}))$

$+ \frac{1}{12}(w_e(\{1,3,4\}) + w_e(\{1,3,5\}) + w_e(\{1,3,6\}) + w_e(\{1,3,7\}) + w_e(\{1,4,5\})$

$\qquad + w_e(\{1,4,6\}) + w_e(\{1,4,7\}) + w_e(\{1,5,6\}) + w_e(\{1,5,7\}) + w_e(\{1,6,7\})$

$\qquad + w_e(\{2,3,4\}) + w_e(\{2,3,5\}) + w_e(\{2,3,6\}) + w_e(\{2,3,7\}) + w_e(\{2,4,5\})$

$\qquad + w_e(\{2,4,6\}) + w_e(\{2,4,7\}) + w_e(\{2,5,6\}) + w_e(\{2,5,7\}) + w_e(\{2,6,7\}))$

$- \frac{1}{12}(w_e(\{3,4,5\}) + w_e(\{3,4,6\}) + w_e(\{3,4,7\}) + w_e(\{3,5,6\}) + w_e(\{3,5,7\}) + w_e(\{3,6,7\})$

$\qquad + w_e(\{4,5,6\}) + w_e(\{4,5,7\}) + w_e(\{4,6,7\}) + w_e(\{5,6,7\}))$

Case $S = \{1\}$:

$\text{Vol}_{G_e}(\partial\{1\})$

$= w_e(\{1\}) - \frac{1}{3}(w_e(\{2\}) + w_e(\{3\}) + w_e(\{4\}) + w_e(\{5\}) + w_e(\{6\}) + w_e(\{7\}))$

$+ \frac{1}{3}(w_e(\{1,2\}) + w_e(\{1,3\}) + w_e(\{1,4\}) + w_e(\{1,5\}) + w_e(\{1,6\}) + w_e(\{1,7\}))$

$- \frac{2}{15}(w_e(\{2,3\}) + w_e(\{2,4\}) + w_e(\{2,5\}) + w_e(\{2,6\}) + w_e(\{2,7\}) + w_e(\{3,4\})$

$\qquad + w_e(\{3,5\}) + w_e(\{3,6\}) + w_e(\{3,7\}) + w_e(\{4,5\}) + w_e(\{4,6\})$

$\qquad + w_e(\{4,7\}) + w_e(\{5,6\}) + +w_e(\{5,7\}) + w_e(\{6,7\}))$

$+ \frac{2}{15}(w_e(\{1,2,3\}) + w_e(\{1,2,4\}) + w_e(\{1,2,5\}) + w_e(\{1,2,6\}) + w_e(\{1,2,7\}) + w_e(\{1,3,4\})$

$\qquad + w_e(\{1,3,5\}) + w_e(\{1,3,6\}) + w_e(\{1,3,7\}) + w_e(\{1,4,5\}) + w_e(\{1,4,6\})$

$\qquad + w_e(\{1,4,7\}) + w_e(\{1,5,6\})) + w_e(\{1,5,7\}) + +w_e(\{1,6,7\})$

$$v_1 = 1,\ v_2, v_3 \in \{2, 3, 4, 5, 6, 7\},\ w_e(\{v_1, v_2\}) + w_e(\{v_1, v_3\}) \ge w_e(\{v_2\}) + w_e(\{v_3\})$$
$$v_1 = 1,\ v_2, v_3, v_4, v_5 \in \{2, 3, 4, 5, 6, 7\},$$
$$w_e(\{v_1, v_2, v_3\}) + w_e(\{v_1, v_4, v_5\}) \ge w_e(\{v_2, v_3\}) + w_e(\{v_4, v_5\})$$
$$\implies \mathrm{Vol}_{G_e}(\partial\{1\}) \ge w_e(\{1\}).$$

$$v_1 = 1,\ v_2 \in \{2, 3, 4, 5, 6, 7\},\ w_e(\{v_1, v_2\}) \le w_e(\{v_1\}) + w_e(\{v_2\})$$
$$v_1 = 1,\ v_2, v_3 \in \{2, 3, 4, 5, 6, 7\},\ w_e(\{v_1, v_2, v_3\}) \le w_e(\{v_1\}) + w_e(\{v_2, v_3\})$$
$$\implies \mathrm{Vol}_{G_e}(\partial\{1\}) \le 5 w_e(\{1\}).$$

Case $S = \{1, 2\}$:

$$\mathrm{Vol}_{G_e}(\partial\{1, 2\})$$
$$= \frac{1}{3}(w_e(\{1\}) + w_e(\{2\})) - \frac{7}{15}(w_e(\{3\}) + w_e(\{4\}) + w_e(\{5\}) + w_e(\{6\}) + w_e(\{7\}))$$
$$+ w_e(\{1, 2\}) - \frac{1}{10}(w_e(\{3, 4\}) + w_e(\{3, 5\}) + w_e(\{3, 6\}) + w_e(\{3, 7\}) + w_e(\{4, 5\})$$
$$+ w_e(\{4, 6\}) + w_e(\{4, 7\}) + w_e(\{5, 6\}) + w_e(\{5, 7\}) + w_e(\{6, 7\}))$$
$$+ \frac{7}{15}(w_e(\{1, 2, 3\}) + w_e(\{1, 2, 4\}) + w_e(\{1, 2, 5\}) + w_e(\{1, 2, 6\} + w_e(\{1, 2, 7\}))$$
$$- \frac{1}{30}(w_e(\{1, 3, 4\}) + w_e(\{1, 3, 5\}) + w_e(\{1, 3, 6\}) + w_e(\{1, 3, 7\}) + w_e(\{1, 4, 5\})$$
$$+ w_e(\{1, 4, 6\}) + w_e(\{1, 4, 7\}) + w_e(\{1, 5, 6\}) + w_e(\{1, 5, 7\}) + w_e(\{1, 6, 7\})$$
$$+ w_e(\{2, 3, 4\}) + w_e(\{2, 3, 5\}) + w_e(\{2, 3, 6\}) + w_e(\{2, 3, 7\}) + w_e(\{2, 4, 5\})$$
$$+ w_e(\{2, 4, 6\}) + w_e(\{2, 4, 7\}) + w_e(\{2, 5, 6\}) + w_e(\{2, 5, 7\}) + w_e(\{2, 6, 7\}))$$
$$+ \frac{1}{6}(w_e(\{3, 4, 5\}) + w_e(\{3, 4, 6\}) + w_e(\{3, 4, 7\}) + w_e(\{3, 5, 6\}) + w_e(\{3, 5, 7\}) + w_e(\{3, 6, 7\})$$
$$+ w_e(\{4, 5, 6\}) + w_e(\{4, 5, 7\}) + w_e(\{4, 6, 7\}) + w_e(\{5, 6, 7\}))$$

$$v_1, v_2 \in \{1, 2\},\ v_3, v_4, v_5, v_6, v_7 \in \{3, 4, 5, 6, 7\},\ w_e(\{v_2, v_6, v_7\}) \le w_e(\{v_1\}) + w_e(\{v_3, v_4, v_5\})$$
$$v_1 = 1, v_2 = 2, v_3, v_4, v_5, v_6, v_7 \in \{3, 4, 5, 6, 7\},$$
$$w_e(\{v_6, v_7\}) \le w_e(\{v_1, v_2, v_3\}) + w_e(\{v_3, v_4, v_5\}) - w_e(\{v_3\})$$
$$v_1 = 1, v_2 = 2, v_3, v_4 \in \{3, 4, 5, 6, 7\},\ w_e(\{v_3\}) + w_e(\{v_4\}) \le w_e(\{v_1, v_2, v_3\}) + w_e(\{v_1, v_2, v_4\})$$
$$\implies \mathrm{Vol}_{G_e}(\partial\{1, 2\}) \ge w_e(\{1, 2\}).$$

$$v_1 = 1,\ v_2 = 2,\ v_3 \in \{3, 4, 5, 6\},\ w_e(\{v_3\}) \ge w_e(\{v_1, v_2, v_3\}) - w_e(\{v_1, v_2\})$$
$$v_1 = 1,\ v_2 = 2,\ v_3, v_4, v_5, v_6, v_7 \in \{3, 4, 5, 6\}, w_e(\{v_3, v_4\}) \ge w_e(\{v_5, v_6, v_7\}) - w_e(\{v_1, v_2\})$$
$$v_1,\ v_2 \in \{1, 2\},\ v_3, v_4, v_5, v_6, v_7 \in \{3, 4, 5, 6\},$$
$$w_e(\{v_1, v_3, v_4\}) \ge w_e(\{v_5, v_6, v_7\}) + w_e(\{v_1\}) - w_e(\{v_1, v_2\})$$
$$\implies \mathrm{Vol}_{G_e}(\partial\{1, 2\}) \le 5 w_e(\{1, 2\}).$$

18

Case $S = \{1, 2, 3\}$**:**

$\mathrm{Vol}_{G_e}(\partial\{1, 2, 3\})$

$= -\dfrac{2}{15}(w_e(\{1\}) + w_e(\{2\}) + w_e(\{3\})) - \dfrac{2}{5}(w_e(\{4\}) + w_e(\{5\}) + w_e(\{6\}) + w_e(\{7\}))$

$+\dfrac{7}{15}(w_e(\{1, 2\}) + w_e(\{1, 3\}) + w_e(\{2, 3\})$

$-\dfrac{1}{6}(w_e(\{1, 4\}) + w_e(\{1, 5\}) + w_e(\{1, 6\}) + w_e(\{1, 7\}) + w_e(\{2, 4\}) + w_e(\{2, 5\})$

$\quad + w_e(\{2, 6\}) + w_e(\{2, 7\}) + w_e(\{3, 4\}) + w_e(\{3, 5\}) + w_e(\{3, 6\}) + w_e(\{3, 7\}))$

$+\dfrac{1}{10}(w_e(\{4, 5\}) + w_e(\{4, 6\}) + w_e(\{4, 7\}) + w_e(\{5, 6\}) + w_e(\{5, 7\}) + w_e(\{6, 7\}))$

$+w_e(\{1, 2, 3\}) + \dfrac{2}{15}(w_e(\{1, 2, 4\}) + w_e(\{1, 2, 5\}) + w_e(\{1, 2, 6\}) + w_e(\{1, 2, 7\})$

$\quad + w_e(\{1, 3, 4\}) + w_e(\{1, 3, 5\}) + w_e(\{1, 3, 6\}) + w_e(\{1, 3, 7\})$

$\quad + w_e(\{2, 3, 4\}) + w_e(\{2, 3, 5\}) + w_e(\{2, 3, 6\}) + w_e(\{2, 3, 7\})$

$-\dfrac{1}{30}(w_e(\{1, 4, 5\}) + w_e(\{1, 4, 6\}) + w_e(\{1, 4, 7\}) + w_e(\{1, 5, 6\}) + w_e(\{1, 5, 7\}) + w_e(\{1, 6, 7\})$

$\quad + w_e(\{2, 4, 5\}) + w_e(\{2, 4, 6\}) + w_e(\{2, 4, 7\}) + w_e(\{2, 5, 6\}) + w_e(\{2, 5, 7\}) + w_e(\{2, 6, 7\})$

$\quad + w_e(\{3, 4, 5\}) + w_e(\{3, 4, 6\}) + w_e(\{3, 4, 7\}) + w_e(\{3, 5, 6\}) + w_e(\{3, 5, 7\}) + w_e(\{3, 6, 7\}))$

$+\dfrac{1}{2}(w_e(\{4, 5, 6\}) + w_e(\{4, 5, 7\}) + w_e(\{4, 6, 7\}) + w_e(\{5, 6, 7\}))$

$v_1, v_2, v_3 \in \{1, 2, 3\},\ w_e(\{v_1\}) + w_e(\{v_2\}) \le w_e(\{v_1, v_3\}) + w_e(\{v_2, v_3\}),$

$v_1, v_2, v_3 \in \{1, 2, 3\},\ v_4, v_5, v_6, v_7 \in \{4, 5, 6, 7\},$

$\qquad\qquad\qquad w_e(\{v_4\}) \le w_e(\{v_1, v_2, v_4\}) + w_e(\{v_4, v_5, v_6\}) - w_e(\{v_3, v_7\}),$

$v_1, v_2, v_3 \in \{1, 2, 3\},\ v_4, v_5, v_6, v_7 \in \{4, 5, 6, 7\},\ w_e(\{v_3, v_7\}) \le w_e(\{v_1, v_2\}) + w_e(\{v_4, v_5, v_6\}),$

$v_1, v_2, v_3 \in \{1, 2, 3\},\ v_4, v_5, v_6, v_7 \in \{4, 5, 6, 7\},\ w_e(\{v_1, v_4, v_5\}) \le w_e(\{v_2, v_3\}) + w_e(\{v_6.v_7\}),$

$\qquad\qquad\qquad\qquad \implies \quad \mathrm{Vol}_{G_e}(\partial\{1, 2, 3\}) \ge w_e(\{1, 2, 3\}).$

$v_1, v_2, v_3 \in \{1, 2, 3\},\ v_4, v_5, v_6, v_7 \in \{4, 5, 6, 7\},$

$\qquad\qquad\qquad w_e(\{v_1, v_4, v_5\}) \ge w_e(\{v_2, v_3\}) + w_e(\{v_4, v_5\}) - w_e(\{v_1, v_2, v_3\}),$

$v_1, v_2, v_3 \in \{1, 2, 3\},\ v_4, v_5, v_6, v_7 \in \{4, 5, 6, 7\},$

$\qquad\qquad\qquad w_e(\{v_1, v_4\}) \ge w_e(\{v_1\}) + w_e(\{v_5, v_6, v_7\}) - w_e(\{v_1, v_2, v_3\}),$

$v_1, v_2 \in \{1, 2, 3\},\ v_3 \in \{4, 5, 6, 7\},\ w_e(\{v_3\}) \ge w_e(\{v_1, v_2, v_3\}) - w_e(\{v_1, v_2\}),$

$v_1, v_2, v_3 \in \{1, 2, 3\},\ w_e(\{v_1\}) \ge w_e(\{v_2, v_3\}) - w_e(\{v_1, v_2, v_3\}),$

$\qquad\qquad\qquad\qquad \implies \quad \mathrm{Vol}_{G_e}(\partial\{1, 2, 3\}) \le 6w_e(\{1, 2, 3\}).$

E Proof of Theorem 3.4

Suppose that $\{f^o_{v\tilde{v}}\}_{\{v\tilde{v} \in E^{(e)}\}} and\, \beta^o$ represent the optimal solution of the optimization problem (11). To prove that the values of β^o are equal to those listed in Table 1, we proceed as follows. The result of the optimization procedure over $\{f_{v\tilde{v}}\}_{\{v\tilde{v} \in E^{(e)}\}}$ produces the weights (coefficients) of the linear mapping. The optimization problem (11) may be rewritten as

$$\min_{\{f_{v\tilde{v}}\}_{\{v, \tilde{v}\} \in E_o}} \quad \beta \tag{20}$$

$$\text{s.t.} \quad w_e(S) \le \sum_{v \in S, \tilde{v} \in e/S} f_{v\tilde{v}}(w_e) \le \beta w_e(S), \quad \forall\, S \in 2^e \text{ and submodular } w_e(\cdot).$$

which is essential a linear programming. However, as there are uncountable many choices for the submodular functions $w_e(\cdot)$, the above optimization problem has uncountable many constraints.

However, given a finite collection of inhomogenous cost functions $\Omega = \{w_e^{(1)}(\cdot), w_e^{(2)}(\cdot), ...\}$ all of which are submodular, the following linear program

$$\min_{\{f_{v\tilde{v}}\}_{\{v,\tilde{v}\}\in E_o}} \beta \qquad\qquad\qquad\qquad\qquad\qquad\qquad\qquad (21)$$

$$\text{s.t.} \quad w_e^{(r)}(S) \leq \sum_{v\in S, \tilde{v}\in e/S} f_{v\tilde{v}}(w_e^{(r)}) \leq \beta w_e^{(r)}(S), \quad \text{for all } S \in 2^e \text{ and } w_e^{(r)}(\cdot) \in \Omega.$$

can be efficiently computed and yields an optimal β^Ω that provides a lower bound for β^o. Therefore, we just need to identify the sets Ω for different values of $\delta(e)$ that meet the values of $\beta^{(e)}$ listed in Table 1.

The proof involves solving the linear program (21). We start by identifying some structural properties of the problem.

Proposition E.1. Given $\delta(e)$, the optimization problem (11) over $\{f_{v\tilde{v}}\}_{\{v\tilde{v}\in E^{(e)}\}}$ involves $3[\frac{\delta(e)}{2}]-1$ variables, where $[a]$ denotes the largest integer not greater than a.

Proof. The linear mapping $f_{v\tilde{v}}$ may be written as

$$f_{v\tilde{v}}(w_e) = \sum_{S\in 2^e} \phi(v\tilde{v}, S)w_e(S),$$

where $\phi(v\tilde{v}, S)$ represent the coefficients that we wish to optimize, and which depend on the edge $v\tilde{v}$ and the subset S. Although we have $\binom{\delta(e)}{2} \times 2^{\delta(e)}$ coefficients, the coefficients are not independent from each other. To see what kind of dependencies exist, define the set of all permutations of the vertices of e $\pi : e \rightarrow \{1, 2, ..., \delta(e)\}$; clearly, there are $\delta(e)!$ such permutations π. Also, define $\pi(S) = \{\pi(v)|v \in S\}$ for $S \subseteq e$. If a set function $w(\cdot)$ over all the subsets of $\{1, 2, ..., \delta(e)\}$ satisfies the following conditions

$$\begin{aligned} w(\emptyset) &= 0, \\ w(S) &= w(\bar{S}), \\ w(S_1) + w(S_2) &\geq w(S_1 \cap S_2) + w(S_1 \cup S_2), \end{aligned}$$

for $S, S_1, S_2 \subseteq \{1, 2, ..., \delta(e)\}$, then one may construct $\delta(e)!$ many inhomogeneous cost functions $w_e^{(\pi)}(\cdot)$ such that for all distinct π one has $w_e^{(\pi)}(\cdot) = w(\pi(\cdot))$. As all the weights $w_e^{(\pi)}$ are submodular and appear in the constraints of the optimization problem (20), the coefficients $\phi(v\tilde{v}, S)$ will be invariant under the permutations π; thus, they will depend only on two parameters, $|\{v, \tilde{v}\} \cap S|$ and $|S|$. We replace ϕ with another function $\tilde{\phi}$ to capture this dependence

$$\phi(v\tilde{v}, S) = \phi(\pi(v)\pi(\tilde{v}), \pi(S)) = \tilde{\phi}(|\{v, \tilde{v}\} \cap S|, |S|).$$

Moreover, as $w_e(S)$ is symmetric, i.e., as $w_e(S) = w_e(\bar{S})$, we also have

$$\tilde{\phi}(|\{v, \tilde{v}\} \cap \bar{S}|, |\bar{S}|) = \tilde{\phi}(|\{v, \tilde{v}\} \cap S|, |S|).$$

Hence, for any given $\delta(e)$, the set of the coefficients of the linear function may be written as

$$\Phi = \{\tilde{\phi}(r, s)|(r, s) \in \{0, 1, 2\} \times \{1, 2, 3, ..., \delta(e) - 2, \delta(e) - 1\}/\{(2, 1), (0, \delta(e) - 1)\},$$

$$\text{s.t.} \quad \tilde{\phi}(0, s) = \tilde{\phi}(2, \delta(e) - s) \,, \, \tilde{\phi}(1, s) = \tilde{\phi}(1, \delta(e) - s)\}.$$

which concludes the proof. $\qquad\square$

Using Proposition E.1, we can transform the optimization problem (21) into the following form:

$$\min_{\Phi} \quad \beta$$

$$\text{s.t. } w_e^{(r)}(S) \leq \sum_{v\in S, \tilde{v}\in e/S} \sum_{S'\subseteq e} \tilde{\phi}(|\{v, \tilde{v}\} \cap S'|, |S'|)w_e^{(r)}(S') \leq \beta w_e^{(r)}(S), \, \forall S \in 2^e, \forall w_e^{(r)}(\cdot) \in \Omega.$$

For a given $\delta(e)$, we list the sets $\Omega = \{w_e^{(1)}, w_e^{(2)}, ...\}$ in Table. 6. The above linear program yields optimal values of β^Ω equal to those listed in Table 1. As already pointed out, the cases $\delta(e) = 2, 3$ are simple to verify, and hence we concentrate on the sets Ω for $\delta(e) \geq 4$. The case $\delta(e) = 7$ is handled similarly but requires a large verification table that we omitted for succinctness.

F   Complexity analysis

Recall that the proposed algorithm consists of three computational steps: 1) Projecting each InH-hyperedge onto a subgraph; 2) Combining the subgraphs to create a graph; 3) Performing spectral clustering on the derived graph based on Algorithm 1 (Appendix. B). The complexity of the algorithms depends on the complexity of these three steps. Let $\delta^* = \max_{e \in E} \delta(e)$ denote the largest size of a hyperedge. If in the first step we solve the optimization procedure (5) for all InH-hyperedges with at most $2^{\delta(e)}$ constraints, the worst case complexity of the algorithm is $O(2^{c\delta^*}|E|)$, where c is a constant that depends on the LP-solver. The second step has complexity $O((\delta^*)^2|E|)$, while the third step has complexity $O(n^2)$, given that one has to find the eigenvectors corresponding to the extremal eigenvalues. Other benchmark hypergraph clustering algorithms, such as Clique Expansion, Star Expansion [11] and Zhou's normalized hypergraph cut [13] share two steps of our procedure and hence have the same complexity for the corresponding computations. In practice, we usually deal with hyperedges of small size (< 10) and hence δ^* may, for all purposes, be treated as a constant. Hence, the complexity overhead of our method is of the same order as that of the last two steps, and hence we retain the same order of computation as classical homogeneous clustering methods. Nevertheless, to reduce the complexity of InH-partition, one may use predetermined mappings of the form (9) and (10). In the applications discussed in what follows, we exclusively used this computationally efficient approach.

G   Discussion of Equation (9)

For the case that only the values of $w_e(\{v\})$ are known, we showed that one may perform perfect projections with $\beta^{(e)} = 1$. Suppose now that $w^{(e)}$ takes the form (9), i.e., that for each pair of vertices $v\tilde{v}$ in e, one has

$$w_{v\tilde{v}}^{(e)} = \frac{1}{\delta(e) - 2} \left[w_e(\{v\}) + w_e(\{\tilde{v}\}) \right] - \frac{1}{(\delta(e) - 1)(\delta(e) - 2)} \sum_{v' \in e} w_e(\{v'\}).$$

For all $v \in e$, one can compute

$$\sum_{\tilde{v} \in e/\{v\}} w_{v\tilde{v}}^{(e)} = \frac{\delta(e) - 1}{\delta(e) - 2} w_e(\{v\}) + \frac{1}{\delta(e) - 2} \sum_{\tilde{v} \in e/\{v\}} w_e(\{\tilde{v}\}) - \frac{1}{\delta(e) - 2} \sum_{v' \in e} w_e(\{v'\})$$
$$= w_e(\{v\},$$

which confirms that the projection is perfect. When $\delta(e) > 3$, a perfect projection is not unique as the problem is underdetermined. It is also easy to check the conditions for nonnegativity of the components of $w^{(e)}$: For each pair of vertices $v\tilde{v}$ in e, one requires

$$w_e(\{v\}) + w_e(\{\tilde{v}\}) \geq \frac{1}{(\delta(e) - 1)} \sum_{v' \in e} w_e(\{v'\}), \tag{22}$$

which indicates the weights in $w_e(\cdot)$ associated with different vertices should satisfy a special form of a balancing condition.

H   Supplementary Applications and Experiments

H.1   Structure Learning of Ranking Data

Synthetic data. We first compare the InH-partition (InH-Par) method with the AnchorsPartition (APar) technique proposed in [26] on synthetic data. Note that APar is assumed to know the correct size of the riffled-independent sets while InH-partition automatically determines the sizes of the parts. We set the number elements to $n = 16$, and partitioned them into a pair $(S^*, \bar{S}^*)$, where $|S^*| = q$, $1 \leq q \leq n$. For a sample set size m, we first independently choose scores $s_i, \bar{s}_i \sim$Uniform([0,1]). For $i \in V$ and then generate m rankings via the following procedure: We first use the Plackett-Luce Model [29] with parameters $s_i, i \in S^*$ and $\bar{s}_i, i \in \bar{S}^*$, to generate σ_{S^*} and $\sigma_{\bar{S}^*}$. Then, we interleave σ_{S^*} and $\sigma_{\bar{S}^*}$, which were sampled uniformly at random without replacement, to form σ. The performance of the method is characterized via the success rate of full recovery of $(S^*, \bar{S}^*)$.
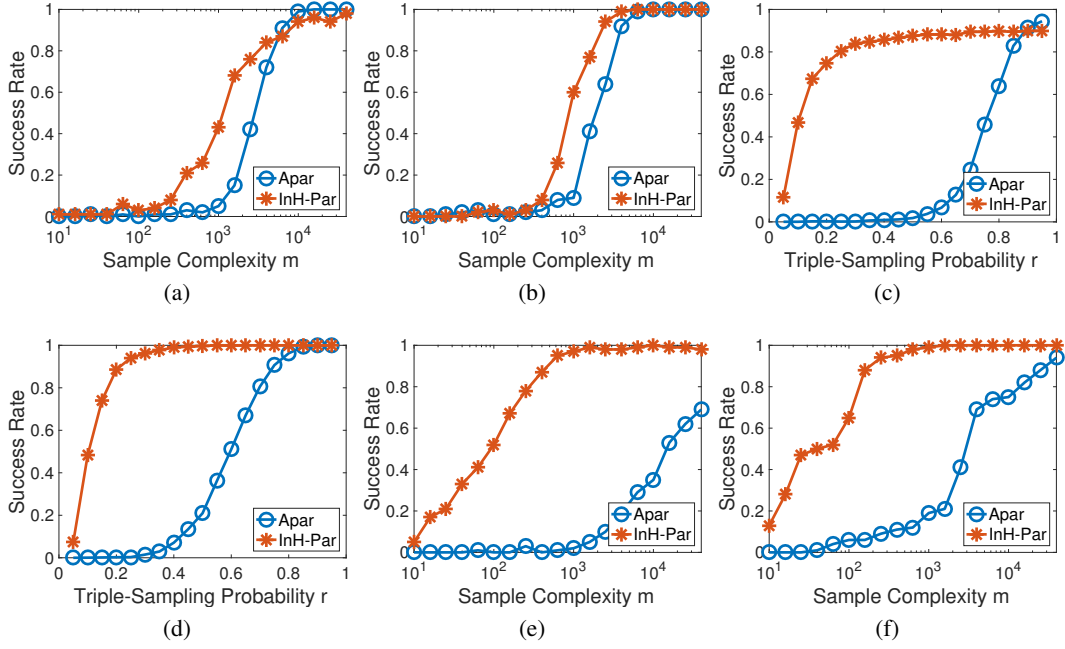
Figure 4: Success rate vs Sample Complexity & Triple-sampling Rate. a),c): $q = 4$ with scores s_i; b),d): $q = 8$ with scores s_i; e) $q = 4$ with scores s_i^3; f): $q = 8$ with scores s_i^3.

The results of various algorithms based on 100 independently generated sample sets are listed in Figure 4 a) and b). For almost all m, InH-partition outperforms APar. Only when $q = 4$ and the sample size m is large, InH-partition may offer worse performance than Apar. The explanation for this finding is that InH-partition performs a normalized cut that tends to balance the sizes of different classes. With regards to the computational complexity of the methods, both require one to evaluate the mutual information of all triples of elements at the cost of $O(mn^3)$ operations. To reduce the time complexity of this step, one may sample each triple independently with probability r. Results pertaining to triple-sampling with $m = 10^4$ are summarized in Figure 4 c) and d). The InH-partition can achieve high success rate 80% even when only a small fraction of triples ($r < 0.2$) is available. On the other hand, APar only works when almost all triples are sampled ($r > 0.7$).

To further test the performance of InH-partition, instead of using the previously described s_i values as the parameters for Plakett-Luce Model, we use the values s_i^3 instead. This choice of parameters further restricts the positions of the candidates within S^* and $\bar{S}^*$. Hence, the mutual information of interest is closer to zero and hence harder to estimate. The results for this setting are shown in part e) and f) of Figure 4. As may be seen, in this setting, the performance of APar is poor while that of InH-partition changes little.

Real data - Supplement for the Irish Election Dataset [27]. The Irish Election Dataset consists of rankings of 14 candidates from different parties, listed in Table 2. This information was used to perform the learning tasks described in the main text.

Table 2: List of candidates from the Meath Constituency Election in 2002 (reproduced from [26, 27])

	Candidate	Party		Candidate	Party
1	Brady, J.	Fianna Fáil	8	Kelly, T.	Independent
2	Bruton, J.	Fine Gael	9	O'Brien, P.	Independent
3	Colwell, J.	Independent	10	O'Byrne, F.	Green Party
4	Dempsey, N.	Fianna Fáil	11	Redmond, M.	Christian Solidarity
5	English, D.	Fine Gael	12	Reilly, J.	Sinn Féin
6	Farrelly, J.	Fine Gael	13	Wallace, M.	Fianna Fáil
7	Fitzgerald, B.	Independent	14	Ward, P.	Labour

22

Table 3: List of 10 sushi from the sushi preference dataset (reproduced from [30])

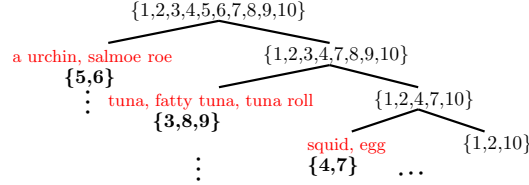|	Sushi	Type		Candidate	Party
1	ebi	shrimp	6	sake	salmon roe
2	anago	sea eel	7	tamago	egg
3	maguro	tuna	8	toro	fatty tuna
4	ika	squid	9	tekka-maki	tuna roll
5	uni	sea urchin	10	kappa-maki	cucumber roll

Figure 5: Hierarchical partitioning structure of sushi preference detected by InH-Par

In addition, we performed the same structure learning task on the sushi preference ranking dataset [30]. This dataset consists of 5000 full rankings of ten types of sushi. The different types of sushi evaluated are listed in Table 3. We ran InH-partition to split the ten sushi types to obtain a hierarchical clustering structure as the one shown in Figure 5. The figure reveals two meaningful clusters, $\{5, 6\}$ (uni,sake) and $\{3, 8, 9\}$ (tuna-related sushi): The sushi types labeled by 5 and 6 have the commonality of being expensive and branded as "daring, luxury sushi," while sushi types labeled by $3, 8, 9$ all contain tuna. InH-partition cannot detect the so-called "vegeterian-choice sushi" cluster $\{7, 10\}$, which was recovered by Apar [26]. This may be a consequence of the ambiguity and overlap of clusters, as the cluster $\{4, 7\}$ may also be categorized as "rich in lecithin". The detailed comparisons between InH-partition and APar are performed based on their ability to detect the two previously described standard clusters, $\{5, 6\}$ and $\{3, 8, 9\}$, using small training sets. The averaged results based on 100 independent tests are depicted in Figure 6 a). As may be seen, InH-partition outperforms APar in recovering both the clusters (uni,sake) and (tuna sushi), and hence is superior to APar when learning both classes simultaneously. We also compared InH-partition and APar in the large sample regime ($m = 5000$) while using only a subset of triples. The averaged results over 100 sets of independent samples are shown Figure 6 b), again indicating the robustness of InH-partition to missing triple information.

H.2 Subspace segmentation

Subspace segmentation is an extension of traditional data segmentation problems that has the goal to partition data according to their intrinsically embedded subspaces. Among subspace segmentation methods, those based on hypergraph clustering exhibit superior performance compared to others [31]. They also exhibit other distinguishing features, such as loose dependence on the choice of parameters [11], robustness to outliers [3, 5], and clustering robustness and accuracy [12].

Hypergraph clustering algorithms are exclusively homogeneous: If the intrinsic affine space is p-dimensional (p-D), the algorithms use ψ-uniform ($\psi > p + 1$, typically set to $p + 2$) hypergraphs $\mathcal{H} = (V, E)$, where the vertices in V correspond to observed data vectors and the hyperedges in E are chosen ψ-tuples of vertices. To each hyperedge e in the hypergraph $\mathcal{H}$ one assigns a weight w_e, typically of the form $w_e = \exp(-d_e^2/\theta^2)$, where d_e describes the deviation needed to fit the corresponding ψ-tuple of vectors into a p-D affine subspace, and θ represents a tunable parameter obtained by cross validation [11] or computed empirically [12]. A small value of d_e corresponds to a large value of w_e, and indicates that ψ-tuples of vectors in e tend to be clustered together. As a good fit of the subspace yields a large weight for the corresponding hyperedge, hypergraph clustering tends to avoid cutting hyperedges of large weight and thus mostly groups vectors within one subspace together. The performance of the methods varies due to different techniques used for computing the deviation d_e and for sampling the hyperedges. Some widely used deviations include $d_e^{\mathrm{H}-1}$, defined as the mean Euclidean distance to the optimal fitted affine subspace [11, 3, 5, 4], and the *polar*
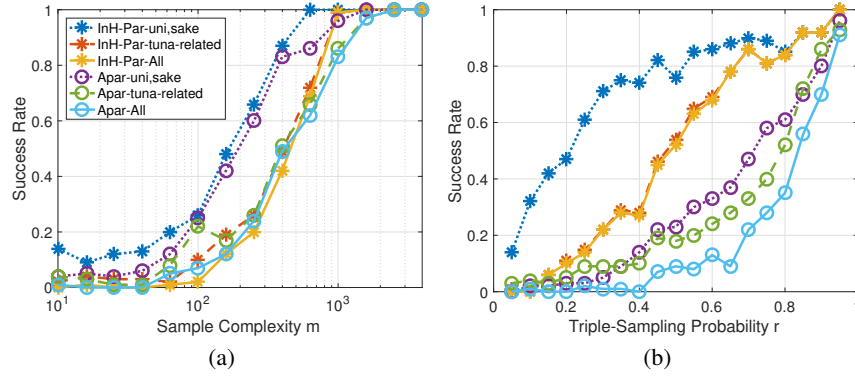
Figure 6: Clusters detected in the sushi preference dataset: a) Success rate vs Sample Complexity; b) Success rate vs Triple-Sampling Probability.

curvature (PC) [12], both of which lead to a homogeneous partition. Instead, we propose to use an inhomogeneous deviation defined as

$$d_e^{\text{InH}}(\{v\}) = \text{Euclidean distance between } v \text{ and the affine subspace generated by } e/\{v\}, \text{ for all } v \in e.$$

This deviation measures the "distance" needed to fit v into the subspace supported by e/v and will be used to construct inhomogeneous cost functions $w_e(\cdot)$ via $w_e(\{v\}) = \exp[-d_e^{\text{InH}}(\{v\})^2/\theta^2]$, as described in what follows. Note that the choice of a "good" deviation is still an open problem, which may depend on specific datasets. Hence, to make a comprehensive comparison, besides $d_e^{\text{H}-1}$ and PC, we also made use of another homogeneous deviation, $d_e^{\text{H}-2} = \sum_{v \in e} d_e^{\text{InH}}(\{v\})/\delta(e)$ which is the average of all the defined inhomogeneous deviations. Comparing the results obtained from d_e^{InH} with $d_e^{\text{H}-2}$ will highlight the improvements obtained from InH-partition, rather than from the choice of the deviation. The inhomogeneous form of deviation $d_e^{\text{InH}}(\cdot)$ has a geometric interpretation based on the polytopes ($p = 1$) shown in Figure 7 (with $d_e^{\text{H}-1}$ and $d_e^{\text{H}-2}$). There, $d_e^{\text{InH}}(\{v\})$ is the distance of $\{v\}$ from the hyperplane spanned by $e/\{v\}$. The induced inhomogeneous weight $w_e(\{v\}) = \exp(-d_e^{\text{InH}}(\{v\})^2/\theta^2)$ may be interpreted as the cost of separating $\{v\}$ away from the other points (vertices) in e.

$$d_e^{\text{H}-1} = (\ell_i + \ell_j + \ell_k)/3$$
$$d_e^{\text{H}-2} = (h_i + h_j + h_k)/3$$
$$d_e^{\text{InH}}(\{v_i\}) = h_i$$
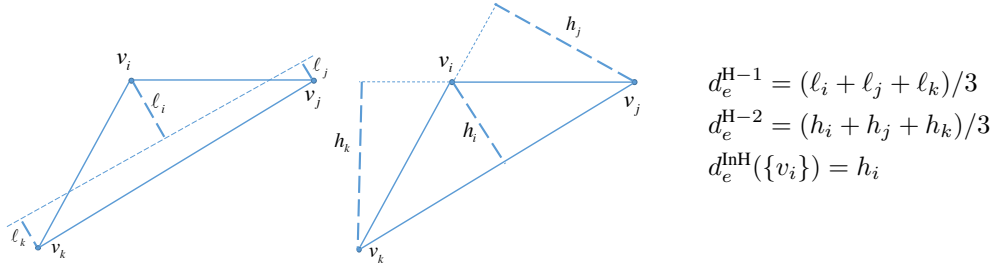
Figure 7: Illustration of the deviation ($p = 1$) used for subspace segmentation.

All hypergraph-partitioning based subspace segmentation algorithms essentially use the NCut procedure described in the main text, but their performances vary due to different approaches for constructing the hypergraphs. Three steps in the clustering procedure are key to the performance quality: The first is to quantify the deviation to fit a collection of vectors into a affine subspace; the second is to choose the parameter θ; the third is to sample ψ-tuples of vectors, i.e., choose the hyperedges of the hypergraph. For fairness of comparison, in all our experiments we computed an inhomogeneous deviation d_e for the hyperedge e instead of a homogeneous one in the first step, and kept the other two key steps the same as used in the standard literature. In particular, we performed hyperedge sampling uniformly at random for the experiments pertaining to k-line segmentation; we used the same hyperedge sampling procedure as that of SCC [12] for the experiments pertaining to motion segmentation. The reason for these two different types of settings are to assess the contribution of InH methods, rather than the sampling procedure.

Table 4: The directions of the k-lines.

k =2	k =3	k =4
(0.97,0.26,0.00) (0.97,-0.26,0.00)	(0.95,0.30,0.00) (0.95,-0.15,0.26) (0.95,-0.15,-0.26)	(0.93,0.37,0.00) (0.93,0.00,0.37) (0.93,-0.37,0.00) (0.93,0.00,-0.37)
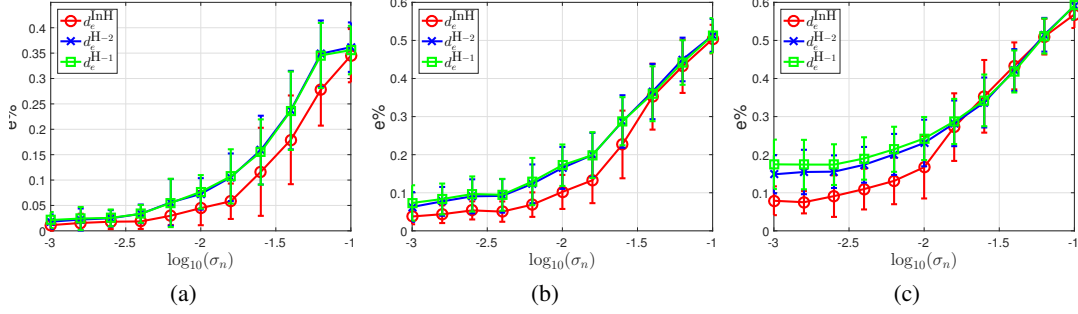
Figure 8: Misclassification rate (mean and standard deviation) vs noise level: a) $k = 2$; b) $k = 3$; c) $k = 4$.

Our first experiment pertains to segmenting k-lines in a 3D Euclidean space ($D = 3, p = 1, k = 2, 3, 4$). The k-lines all pass through the origin, and their directions, listed in Table 4, are such that the minimal angles between two lines are restricted to 30 degree; 40 points are sampled uniformly from the segment of each line lying in the unit ball so there are $40k$ points in total. Each point is independently corrupted by 3D mean-zero Gaussian noise with covariance matrix $\theta_n^2 \mathbf{I}$. We determined the parameter θ through cross validation and uniformly at random picked $100 \times k^2$ many triples. We computed the percentage of misclassified points based on 50 independent tests; the misclassification rate is denoted by $e\%$ and the results are shown in Figure 8. The InH-partition only has 50% of the misclassification errors of H-partition, provided that the noise is small ($\theta_n < 0.01$). To see why this may be the case, let us consider a triple of datapoints $\{v_i, v_j, v_k\}$ where v_i and v_j belong to the same cluster, while v_k may belong to a different cluster. The line that goes through v_i and v_j is close to the true affine subspace when the noise is small and thus the distance from the third point v_k to this line can serve as a precise indicator whether v_k lies within the same true affine subspace. When the noise is high, the InH-partition also performs better when the number of classes is $k = 2$, but starts to deteriorate in performance as k increases. The reason behind this phenomena is as follows: Inhomogenous costs of a hyperedge provide more accurate information about the subspaces than the homogenous costs when at least two points of the hyperedge belong to the same line cluster. This is due to the definition of the deviation d_e^{inH}; but hyperedges of this type become less likely as k increases.

The second problem we investigated in the context of subspace clustering is motion segmentation. Motion segmentation, a widely used application in computer vision, is the task of clustering point trajectories extracted from a video of a scene according to different rigid-body motions. The problem can be reduced to a subspace clustering problem as all the trajectories associated with one motion lie in one specified 3D affine subspace ($p = 3$) [32]. We evaluate the performance of the InH-partition method over the well-known motion segmentation dataset, Hopkins155 [33]. This dataset consists of 155 sequences of two and three motions from three categories of scenes: Checkerboard, traffic and articulated sequences. Our experiments show the InH-partition algorithm outperforms the benchmark algorithms based on the use of H-partitions over this dataset including spectral curvature clustering technique (SCC [12]). To make the comparison fair, we simply replaced the homogeneous distance *polar curvature* in SCC with the inhomogeneous distance d_e^{InH}, the homogenous distances $d_e^{\text{H}-1}$ and $d_e^{\text{H}-2}$, and keep all other steps the same. We also evaluated the performance of some other methods, including Generalized PCA (GPCA) [34], Local Subspace Affinity [35], Agglomerative Lossy Compression (ALC) [36], and Sparse Subspace Clustering (SSC) [37]. The results based on the average over 50 runs for each video are shown in Table 5.

As may be seen, InH-partition outperforms all methods except for SSC (not based on hypergraph clustering), which shows the superiority of replacing H-hyperedges with inhomogeneous ones. Although InH-partition fails to outperform SSC, it has significantly lower complexity and is much easier to use and implement in practice. In addition, some recent algorithms based on H-partitions may leverage the complex hyperedge-sampling steps for this application [38], and we believe that the InH-partition method can be further improved by changing the sampling procedure, and made more appropriate for inhomogeneous hypergraph clustering as opposed to SSC. This topic will be addressed elsewhere.

Table 5: Misclassification rates $e\%$ for the Hopkins 155 dataset. (MN: mean; MD: median)

Method	Two Motions								Three Motions							
	Chck.(78)		Trfc.(31)		Artc.(11)		All(120)		Chck.(26)		Trfc.(7)		Artc.(2)		All(115)	
	MN	MD	MN	MD	MN	MD	MN	MD	MN	MD	MN	MD	MN	MD	MN	MD
GPCA [34]	6.09	1.03	1.41	0.00	2.88	0.00	4.59	0.38	31.95	32.93	19.83	19.55	16.85	16.85	28.66	28.26
LSA [35]	2.57	0.27	5.43	1.48	4.10	1.22	3.45	0.59	5.80	1.77	25.07	23.79	7.25	7.25	9.73	2.33
ALC [36]	1.49	0.27	1.75	1.51	10.70	0.95	2.40	0.43	5.00	0.66	8.86	0.51	21.08	21.08	6.69	0.67
SSC [37]	1.12	0.00	0.02	0.00	0.62	0.00	0.82	0.00	2.97	0.27	0.58	0.00	1.42	1.42	2.45	0.20
SCC [12]	1.77	0.00	0.63	0.14	4.02	2.13	1.68	0.07	6.23	1.70	1.11	1.40	5.41	5.41	5.16	1.58
H+d_e^{H-1}	12.27	5.06	14.91	9.94	12.85	3.66	12.92	6.01	22.13	23.98	21.99	18.12	19.79	19.79	21.97	20.45
H+d_e^{H-2}	4.20	0.43	0.33	0.00	1.53	0.10	2.93	0.06	7.05	2.22	7.02	3.98	6.47	6.47	7.01	2.12
InH-par	1.69	0.00	0.61	0.22	1.22	0.62	1.40	0.04	4.82	0.69	2.46	0.60	4.23	4.23	4.06	0.65

Table 6: Inhomogeous cost functions $w_e^{(r)}(S)$ for $\delta(e) \in \{4,5,6\}$.

$\delta(e) = 4,\ \beta^{(e)} = 3/2$

r	S						
	1	2	3	4	1, 2	1, 3	1, 4
1	0	1	1	1	1	1	1
2	0	0	1	1	0	1	1
3	1	1	1	1	1	1	1
4	1	1	1	1	2	2	2

$\delta(e) = 5,\ \beta^{(e)} = 2$

r	S														
	1	2	3	4	5	1, 2	1, 3	1, 4	1, 5	2, 3	2, 4	2, 5	3, 4	3, 5	4, 5
1	0	1	1	1	1	1	1	1	1	1	1	1	1	1	1
2	0	1	1	1	1	1	1	1	1	2	2	2	2	2	2
3	1	1	1	1	1	1	1	1	1	1	1	1	1	1	1
4	1	1	1	1	1	1	2	2	2	2	2	2	1	1	1
5	1	1	1	1	1	0	2	2	2	2	2	2	1	1	1
6	1	1	1	1	1	2	2	2	2	2	2	2	2	2	2

$\delta(e) = 6,\ \beta^{(e)} = 4$

r	S														
	1	2	3	4	5	6	1, 2	1, 3	1, 4	1, 5	1, 6	2, 3	2, 4	2, 5	2, 6
1	0	1	1	1	1	1	1	1	1	1	1	1	1	1	1
2	0	1	1	1	1	1	1	1	1	1	1	2	2	2	2
3	1	1	1	1	1	1	1	1	1	1	1	1	1	1	1
4	1	1	1	1	1	1	2	2	2	2	2	2	2	2	2
5	1	1	1	1	1	1	1	2	2	2	2	2	2	2	2
6	1	1	1	1	1	1	0	2	2	2	2	2	2	2	2
7	1	1	1	1	1	1	1	1	2	2	2	1	2	2	2
8	1	1	1	1	1	1	2	2	2	2	2	2	2	2	2
9	1	1	1	1	1	1	1	1	2	2	2	1	2	2	2

r	S											
	3, 4	3, 5	3, 6	4, 5	4, 6	5, 6	1, 2, 3	1, 2, 4	1, 2, 5	1, 2, 6	1, 3, 4	1, 3, 5
1	1	1	1	1	1	1	1	1	1	1	1	1
2	2	2	2	2	2	2	2	2	2	2	2	2
3	1	1	1	1	1	1	1	1	1	1	1	1
4	2	2	2	2	2	2	3	3	3	3	3	3
5	1	1	1	1	1	1	1	1	1	1	2	2
6	1	1	1	1	1	1	1	1	1	1	2	2
7	2	2	2	1	1	1	1	2	2	2	2	2
8	2	2	2	2	2	2	1	3	3	3	3	3
9	2	2	2	1	1	1	0	2	2	2	2	2

r	S			
	1, 3, 6	1, 4, 5	1, 4, 6	1, 5, 6
1	1	1	1	1
2	2	2	2	2
3	1	1	1	1
4	3	3	3	3
5	2	2	2	2
6	2	2	2	2
7	2	2	2	2
8	3	3	3	3
9	2	2	2	2

Table 7: Species in the Florida Bay foodweb with biological classification and assigned clusters. Cluster labels and colors correspond to the clusters shown in Figure 2. For InH-partition, in the first-level clustering, the species Roots is the only singleton while in the second-level clustering, the species Kingfisher, Hawksbill Turtle and Manatee are singletons.

Species	Biological Classification	Cluster (Ours)	Cluster (Benson's [10])
Roots	producers (no predator)	Singleton	Singleton
2μm Spherical cya	phytoplankton producers	Green	Singleton
Synedococcus	phytoplankton producers	Green	Singleton
Oscillatoria	phytoplankton producers	Green	Singleton
Small Diatoms ($< 20\mu$m)	phytoplankton producers	Green	Singleton
Big Diatoms ($> 20\mu$m)	phytoplankton producers	Green	Singleton
Dinoflagellates	phytoplankton producers	Green	Singleton
Other Phytoplankton	phytoplankton producers	Green	Singleton
Free Bacteria	producers	Green	Green
Water Flagellates	producers	Green	Green
Water Cilitaes	producers	Green	Green
Kingfisher	bird (no predator)	Singleton	Singleton
Hawksbill Turtle	reptiles (no predator)	Singleton	Singleton
Manatee	mammal (no predator)	Singleton	Singleton
Rays	fish	Blue	Singleton
Bonefish	fish	Blue	Singleton
Lizardfish	fish	Blue	Red
Catfish	fish	Blue	Blue
Eels	fish	Blue	Red
Brotalus	fish	Blue	Blue
Needlefish	fish	Blue	Yellow
Snook	fish	Blue	Singleton
Jacks	fish	Blue	Singleton
Pompano	fish	Blue	Singleton
Other Snapper	fish	Blue	Singleton
Gray Snapper	fish	Blue	Singleton
Grunt	fish	Blue	Singleton
Porgy	fish	Blue	Singleton
Scianids	fish	Blue	Singleton
Spotted Seatrout	fish	Blue	Singleton
Red Drum	fish	Blue	Singleton
Spadefish	fish	Blue	Singleton
Flatfish	fish	Blue	Blue
Filefish	fish	Blue	Singleton
Puffer	fish	Blue	Singleton
Other Pelagic fish	fish	Blue	Yellow
Small Herons & Egrets	bird	Blue	Singleton
Ibis	bird	Blue	Singleton
Roseate Spoonbill	bird	Blue	Singleton
Herbivorous Ducks	bird	Blue	Singleton
Omnivorous Ducks	bird	Blue	Singleton
Gruiformes	bird	Blue	Singleton
Small Shorebird	bird	Blue	Singleton
Gulls & Terns	bird	Blue	Singleton
Loggerhead Turtle	reptiles (no predator)	Blue	Singleton
Sharks	fish (no predator)	Purple	Singleton
Tarpon	fish	Purple	Singleton
Grouper	fish (no predator)	Purple	Singleton
Mackerel	fish (no predator)	Purple	Singleton
Barracuda	fish	Purple	Singleton
Loon	bird (no predator)	Purple	Singleton
Greeb	bird (no predator)	Purple	Singleton
Pelican	bird	Purple	Singleton
Comorant	bird	Purple	Singleton
Big Herons & Egrets	bird	Purple	Singleton
Predatory Ducks	bird (no predator)	Pubirdrple	Singleton
Raptors	bird (no predator)	Purple	Singleton
Crocodiles	reptiles (no predator)	Purple	Singleton
SingleDolphin	mammal (no predator)	Purple	Singleton

Species	Biological Classification	Cluster Labels	Cluster(Benson's [10])
Benthic microalgea	algea producers	Yellow	Blue
Thalassia	seagrass producers	Yellow	Blue
Halodule	seagrass producers	Yellow	Blue
Syringodium	seagrass producers	Yellow	Blue
Drift Algae	algea producers	Yellow	Blue
Epiphytes	algea producers	Yellow	Blue
Acartia Tonsa	zooplankton invertebrates	Yellow	Green
Oithona nana	zooplankton invertebrates	Yellow	Green
Paracalanus	zooplankton invertebrates	Yellow	Green
Other Copepoda	zooplankton invertebrates	Yellow	Green
Meroplankton	zooplankton invertebrates	Yellow	Green
Other Zooplankton	zooplankton invertebrates	Yellow	Green
Benthic Flagellates	invertebrates	Yellow	Blue
Benthic Ciliates	invertebrates	Yellow	Blue
Meiofauna	invertebrates	Yellow	Blue
Sponges	macro-invertebrates	Yellow	Green
Bivalves	macro-invertebrates	Yellow	Blue
Detritivorous Gastropods	macro-invertebrates	Yellow	Blue
Epiphytic Gastropods	macro-invertebrates	Yellow	Singleton
Predatory Gastropods	macro-invertebrates	Yellow	Blue
Detritivorous Polychaetes	macro-invertebrates	Yellow	Blue
Predatory Polychaetes	macro-invertebrates	Yellow	Blue
Suspension Feeding Polych	macro-invertebrates	Yellow	Blue
Macrobenthos	macro-invertebrates	Yellow	Blue
Benthic Crustaceans	macro-invertebrates	Yellow	Blue
Detritivorous Amphipods	macro-invertebrates	Yellow	Blue
Herbivorous Amphipods	macro-invertebrates	Yellow	Blue
Isopods	macro-invertebrates	Yellow	Blue
Herbivorous Shrimp	macro-invertebrates	Yellow	Red
Predatory Shrimp	macro-invertebrates	Yellow	Blue
Pink Shrimp	macro-invertebrates	Yellow	Blue
Thor Floridanus	macro-invertebrates	Yellow	Singleton
Detritivorous Crabs	macro-invertebrates	Yellow	Red
Omnivorous Crabs	macro-invertebrates	Yellow	Blue
Green Turtle	reptiles	Yellow	Singleton
Coral	macro-invertebrates	Red	Singleton
Other Cnidaridae	macro-invertebrates	Red	Blue
Echinoderma	macro-invertebrates	Red	Blue
Lobster	macro-invertebrates	Red	Singleton
Predatory Crabs	macro-invertebrates	Red	Red
Callinectus sapidus	macro-invertebrates	Red	Red
Stone Crab	macro-invertebrates	Red	Singleton
Sardines	fish	Red	Yellow
Anchovy	fish	Red	Yellow
Bay Anchovy	fish	Red	Yellow
Toadfish	fish	Red	Blue
Halfbeaks	fish	Red	Yellow
Other Killifish	fish	Red	Singleton
Goldspotted killifish	fish	Red	Yellow
Rainwater killifish	fish	Red	Yellow
Sailfin Molly	fish	Red	Singleton
Silverside	fish	Red	Yellow
Other Horsefish	fish	Red	Singleton
Gulf Pipefish	fish	Red	Singleton
Dwarf Seahorse	fish	Red	Singleton
Mojarra	fish	Red	Singleton
Pinfish	fish	Red	Singleton
Parrotfish	fish	Red	Singleton
Mullet	fish	Red	Blue
Blennies	fish	Red	Blue
Code Goby	fish	Red	Red
Clown Goby	fish	Red	Red
Other Demersal Fish	fish	Red	Blue